

# Robust Bayesian Optimization via Tempered Posteriors

Jiguang Li\*

Booth School of Business, University of Chicago

Hengrui Luo†

Department of Statistics, Rice University  
and

Computational Research Division, Lawrence Berkeley National Laboratory

## Abstract

Bayesian optimization (BO) iteratively fits a Gaussian process (GP) surrogate to accumulated evaluations and selects new queries via an acquisition function such as expected improvement (EI). In practice, BO often concentrates evaluations near the current incumbent, causing the surrogate to become overconfident and to underestimate predictive uncertainty in the region guiding subsequent decisions. We develop a robust GP-based BO via tempered posterior updates, which downweight the likelihood by a power  $\alpha \in (0, 1]$  to mitigate overconfidence under local misspecification. We establish cumulative regret bounds for tempered BO under a family of generalized improvement rules, including EI, and show that tempering yields strictly sharper worst-case regret guarantees than the standard posterior ( $\alpha = 1$ ), with the most favorable guarantees occurring near the classical EI choice.

Motivated by our theoretic findings, we propose a prequential procedure for selecting  $\alpha$  online: it decreases  $\alpha$  when realized prediction errors exceed model-implied uncertainty and returns  $\alpha$  toward one as calibration improves. Empirical results demonstrate that tempering provides a practical yet theoretically grounded tool for stabilizing BO surrogates under localized sampling.

*Keywords:* Robust Bayesian Optimization; Online Calibration; Tempered Posteriors; Non-parametric Regression.

---

\*Email: [jiguang@chicagobooth.edu](mailto:jiguang@chicagobooth.edu). Jiguang Li is a 4th-year doctoral student in Econometrics and Statistics at the Booth School of Business of the University of Chicago. The author would like to thank Sean O'Hagan and Veronika Rockova for their valuable inputs for the manuscript.

†Corresponding Author. Email: [h180@rice.edu](mailto:h180@rice.edu)

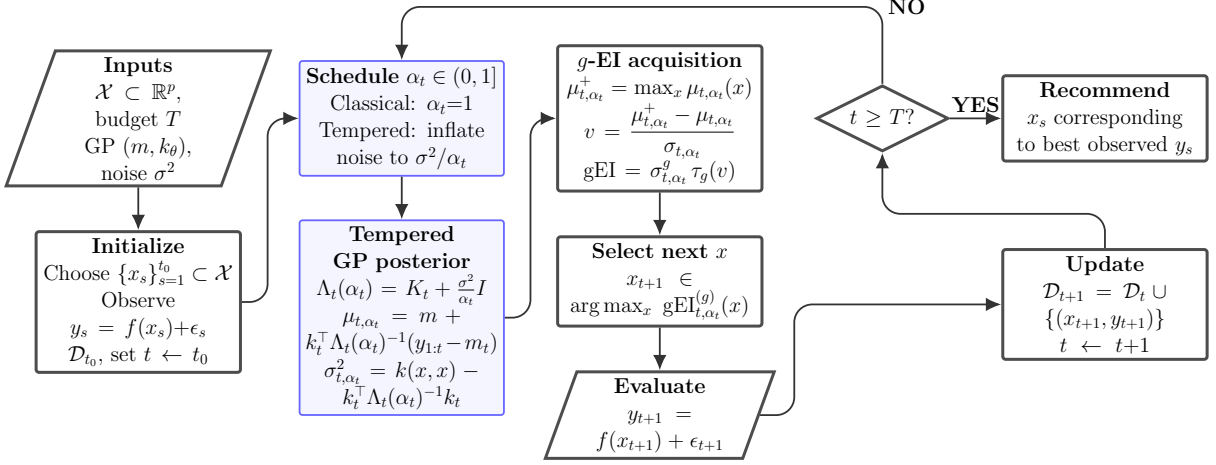


Figure 1: Schematic procedure of BO with possible tempered posterior. The tempered posterior part is indicated by blue boxes, setting  $\alpha_t \equiv 1$  in these blue boxes reduces to the regular BO.

# 1 Introduction

## 1.1 Basic concepts and BO pipeline

Bayesian optimization (BO) aims to identify a global maximizer of an unknown black-box function  $f$  defined on a compact search domain  $\mathcal{X}$  (Garnett, 2023). The algorithm proceeds by sequentially querying an input location  $x_t \in \mathcal{X}$  and observing a noisy response  $y_t = f(x_t) + \varepsilon_t$  from the truth  $f(\cdot) \in \mathbb{R}$  with noise  $\varepsilon_t \sim \mathcal{N}(0, \sigma^2)$ . The datum collected up to time  $t$  is denoted by  $\mathcal{D}_t = \{(x_s, y_s)\}_{s=1}^t$  and the procedure stops until time  $T$ . Based on the datum, we may build a surrogate model summarizes  $\mathcal{D}_t$  and delivers a predictive mean  $\mu_t(\cdot; \theta)$  and a predictive standard deviation  $\sigma_t(\cdot; \theta)$ , where  $\theta$  usually denotes model hyperparameters estimated from  $\mathcal{D}_t$ .

In this work, the surrogate may be a linear model or a Gaussian process (GP) regression. When the algorithm proceeds, the next location  $x_{t+1}$  is selected by maximizing an acquisition function  $\mathcal{A}$  that balances exploration with exploitation and is measurable with respect to  $\mathcal{D}_t$ . The choice of the next location comes from the rule  $x_{t+1} = \arg \max_{x \in \mathcal{X}} \mathcal{A}(x \mid \mathcal{D}_t)$ , where  $\mathcal{A}$  is any acquisition computed from the current surrogate. Figure 1 presents a schematic view of the pipeline where we allow the surrogate update step to employ a *tempered posterior*, in which the likelihood is raised to a fractional power  $\alpha \in (0, 1]$  (Bhattacharya et al., 2019). When  $\alpha_t \equiv 1$ , this procedure is identical to the usual BO pipeline (Garnett, 2023).

## 1.2 Related literature

The foundations of BO trace back to early work on expected improvement and related strategies that use GP surrogates to guide adaptive evaluation (Gramacy, 2020; Moćkus, 1974). Our work focuses on the generalized expected improvement ( $g$ -EI) acquisition functions that interpolate between probability of improvement (PI) and classical expected improvement (EI) (Schonlau et al., 1998). These criteria provide a convenient unifying framework for studying how sensitivity to improvement magnitude influences the exploration-exploitation tradeoff. We note that subsequent development in BO also introduced alternative acquisition principles, including knowledge gradient policies and information based criteria (Frazier et al., 2009; Srinivas et al., 2012). Parallel to this line of work, a substantial BO theory has established cumulative regret guarantees for various acquisition functions, with GP-UCB (Srinivas et al., 2012) serving as a canonical example and motivating many subsequent refinements (Jaiswal et al., 2023). For EI ( $g = 1$ ) in particular, Wang and de Freitas (2014) provided one of the first finite-time cumulative regret analyses by relating EI to information gain.

A central theme of this paper is the robustness of BO updating under model misspecification. One widely studied strategy replaces the usual Bayesian posterior with a likelihood tempered update,

$$p_\alpha(\theta | \mathcal{D}) \propto p(\theta)p(\mathcal{D}|\theta)^\alpha, \quad \alpha \in (0, 1], \quad (1)$$

which downweights the information contributed by each observation. The same construction appears under several names across communities. In the robust Bayesian asymptotics literature it is commonly referred to as a *tempered* (or *fractional*) posterior (Alquier and Ridgway, 2020; Bhattacharya et al., 2019; Pitas and Arbel, 2024; Yang et al., 2020), whereas in computational Bayes and marginal-likelihood estimation it is often called a *power posterior* and used for thermodynamic integration and related evidence estimators (Friel and Pettitt, 2008; Watanabe, 2013). Throughout, we use the term *tempered posterior* to emphasize the role of  $\alpha$  as a temperature/learning-rate parameter.

This perspective connects directly to generalized Bayes, which replaces the log-likelihood with a loss and introduces a learning-rate parameter that controls the update magnitude (Bissiri et al., 2016; Knoblauch et al., 2022; Lyddon et al., 2019; Syring and Martin, 2019). Growing Bayes-PAC theory clarifies why tempering helps under misspecification, from misspecified Bernstein-von Mises guarantees to concentration results for tempered posteriors and their variational approximations (Alquier and Ridgway, 2020; Kleijn and van der Vaart, 2012; Yang et al., 2020). Practical schemes for choosing or adapting the temperature include SafeBayes and related extensions (de Heide et al., 2020; Grünwald, 2012; Grünwald and Van Ommen, 2017), and following works explored exact conditioning with coarsened

or divergence based updates, delivering robustness to small departures from the model (Ghosh and Basu, 2016; Miller and Dunson, 2019).

In terms of BO, to the best of our knowledge, we introduce the tempered posterior for the first time to enhance robustness. A related line of work adapts exploration-exploitation behavior by modifying the acquisition rule itself (Golovin et al., 2017; Srinivas et al., 2009). Classic extensions include noisy and augmented variants of expected improvement that introduce exploration margins or corrections for observation noise (Hu et al., 2025; Huang et al., 2006; Letham et al., 2019). Other approaches adaptively combine multiple acquisitions (Brochu et al., 2010; Shahriari et al., 2014), or adjust internal weighting parameters within improvement-based rules to rebalance exploration over time (Benjamins and Lindauer, 2023; Qin et al., 2017). Recent work revisits acquisition design from a variational-inference perspective, proposing hybrid acquisition rules (Cheng et al., 2025). These methods regulate exploration through acquisition-level tuning or model combination, whereas our approach operates at the surrogate-update level via likelihood tempering, providing a complementary and broadly applicable mechanism for robustly alleviating posterior overconfidence.

### 1.3 Contributions and Organization

Despite these developments illustrated in Section 1.2, existing regret analyses for BO typically assume the standard Bayesian update ( $\alpha = 1$ ), while the robust Bayes literature largely studies tempering outside sequential decision problems. The present paper addresses this gap by analyzing BO under tempered surrogates and deriving regret bounds that make the roles of tempering and the choice of acquisition functions within the generalized improvement family explicit.

Building on these strands, we study BO with tempered surrogate updates and characterize how tempering affects improvement based acquisition functions. Our contributions are threefold. First, we embed likelihood tempering into Bayesian linear and GP surrogates and show how tempering can lead to empirical success in BO. Second, for the generalized improvement family indexed by  $g$  (including PI and EI as special cases), we derive closed-form expressions under the tempered GP surrogate and establish cumulative regret bounds that depend explicitly on  $(\alpha, g)$  through a tempered information-gain term. In the classical EI setting ( $\alpha = 1, g = 1$ ) our analysis yields a sharper logarithmic dependence than existing EI regret bounds (Wang and de Freitas, 2014). Third, motivated by these guarantees, we propose a tuning-light prequential schedule for choosing  $\alpha_t$  at step  $t$  in a fully sequential BO loop and show that it recovers  $\alpha_t \rightarrow 1$  under calibration while converging to a limit under persistent misspecification.

In the rest of the paper, Section 2.1 motivates robustness through the tempered posterior and Section 2.2 provides a concrete toy illustration. Section 3 studies a Bayesian linear

surrogate with tempered posterior, establishes a first regret analysis for tempered posterior in BO setting. Section 4 develops GP surrogates, gives a closed form for the generalized expected improvement, and provides regret bounds as our main theoretic investigation of the tempered posterior in BO setting. Section 5 describes algorithmic design choices, including a tuning-light schedule for adaptively choosing  $\alpha$ . Section 6 reports experimental results on benchmark functions, followed by a concluding discussion in Section 7.

## 2 Motivations

### 2.1 Misspecification and Regret Guarantees

The BO pipeline above highlights a tension between statistical modeling and sequential decision-making with an exception of [Jaiswal et al. \(2023\)](#), where sequential sampling instead of BO acquisition is the focus. Since BO produces an adaptive design ([Srinivas et al., 2009](#)) and often concentrate evaluations near the current incumbent, the surrogate can become predictively overconfident in the sense that its model-implied predictive uncertainty understates realized errors precisely in the region that drives acquisition decisions.

The miscalibration we target is primarily *uncertainty misspecification* rather than global correctness of the surrogate class. It can arise from kernel mismatch (e.g., incorrect smoothness/lengthscale or stationarity imposed on a nonstationary function), noise misspecification (e.g., underestimating  $\sigma^2$ , heteroskedasticity, or heavy-tailed errors), and repeated local refitting on a highly nonuniform design. A standard Bayesian device to alleviate misspecification is the tempered posterior ([Bhattacharya et al., 2019](#)), which raises the likelihood to a power  $\alpha \in (0, 1]$  and thereby downweights the influence of its contributions. For Gaussian noise GP regression, this is roughly equivalent to inflating the effective noise variance from  $\sigma^2$  to  $\sigma^2/\alpha$ , preventing the posterior from collapsing too quickly. Thus, tempering acts directly at the surrogate update step that produces the predictive mean and variance used by the acquisition.

While tempering can mitigate model misspecification and predictive overconfidence, the effect of likelihood tempering on BO performance is not well understood. From a BO perspective, it is unclear whether it can be detrimental to cumulative regret. At the same time, it is well known that the choice of acquisition function plays a central role in BO and can directly influences regret. For instance, PI is more exploitative and can be effective once a promising region has been identified, whereas EI offers a more balanced exploration-exploitation trade-off. To study this interaction between acquisition-level and surrogate-level adaptiveness systematically, we work with the most widely used generalized EI ( $g$ -EI) family ([Schonlau et al., 1998](#)):

$$\alpha_{\theta, g, \alpha}^{EI(f)}(x \mid \mathcal{D}_t) = \mathbb{E} \left[ \left( \max\{0, f(x) - \mu_{\theta_t, \alpha}^+\} \right)^g \mid \mathcal{D}_t \right], \quad g \in \mathbb{R}_{\geq 0}, \quad \alpha \in (0, 1], \quad (2)$$

where  $\mu_{\theta_t, \alpha}^+ := \max_{x \in \mathcal{X}} \mu_{t, \alpha}(x; \theta)$ . Practically, we sometimes introduce jittering  $\xi > 0$  instead of 0 inside the bracket. The algorithm selects the next query point by computing  $x_{t+1} = \arg \max_{x \in \mathcal{X}} \alpha_{\theta, g, \alpha}^{EI(f)}(x | D_t)$ . In the standard posterior setting ( $\alpha = 1$ ), equation (2) reduces to PI when  $g = 0$ , and it recovers classical EI when  $g = 1$ . Larger  $g$  values place greater weight on the magnitude of improvement. In this formulation,  $\alpha$  and  $g$  play distinct and complementary roles:  $\alpha$  controls how aggressively the surrogate trusts the data, while  $g$  controls how the acquisition maps posterior uncertainty into exploration incentives. This family of acquisition functions (2) is moment-based and orthogonal to entropy-based acquisition functions studied in [Cheng et al. \(2025\)](#).

Existing BO regret analyses typically assume a standard Bayesian posterior update ( $\alpha = 1$ ) and do not directly apply once the surrogate is tempered ([Jaiswal et al., 2023](#)), since the predictive variances and the associated information-gain quantities are altered. Motivated by this theoretical gap, we analyze generalized improvement under a tempered predictive distribution and derive regret bounds that explicitly depend on  $\alpha$  and  $g$ . This theory suggests tempering can be beneficial under the popular GP surrogate, and clarifies how tempering and acquisition sensitivity jointly shape exploration and convergence. We further propose a simple prequential schedule for selecting  $\alpha$  in a fully Bayes BO implementation as a novel methodology inspired by our theoretical result.

## 2.2 A Toy Illustration

To provide an intuitive illustration of why likelihood tempering can matter in BO, we consider a simple one-dimensional example designed to highlight a common failure mode of PI: when the surrogate becomes overconfident early, PI can concentrate on a single basin and under-explore competing regions.

Figure 2 visualizes an unknown black-box function with true maximum 1 at  $x = 0$ :

$$f(x) = -2 \frac{\cos(8|4x - 2|)}{|4x - 2|^2 + 2}, \quad x \in [0, 1], \quad (3)$$

observed with Gaussian noise of standard deviation 0.05. We fit a GP surrogate with a Matérn covariance (smoothness fixed to  $\nu = 2$ ) and estimate the remaining hyperparameters, including a white-noise term by marginal likelihood (with multiple restarts). We run PI with jitter  $\xi = 0.01$  under three tempering levels  $\alpha \in \{0.1, 0.5, 1.0\}$ , where  $\alpha = 1$  is the usual posterior. Each choice of  $\alpha$  starts from the same five initial points and then repeatedly selects  $x_{t+1}$  by maximizing PI under the corresponding tempered predictive distribution.

The key mechanism is that tempering reduces the effective influence of each observation in the surrogate update. Since PI depends on standardized improvement, an underestimated predictive variance can make PI sharply peaked around the current incumbent and discourage exploration elsewhere; tempering counteracts this by maintaining non-negligible

uncertainty away from the incumbent and keeping alternative regions competitive.

This behavior is visible in Figure 2. By iteration 10, the tempered run with  $\alpha = 0.1$  has already sampled the region around the global peak and attains a best observed value near 0.968, while the  $\alpha \in \{0.5, 1.0\}$  trajectories remain around 0.819 and 0.817. The corresponding PI curves show that smaller  $\alpha$  produces broader, less brittle acquisition profiles, whereas larger  $\alpha$  yields more concentrated peaks that can reinforce repeated sampling in the same basin. This example illustrates that tempering can restore exploration to PI when the surrogate becomes locally overconfident under adaptive sampling. Additional toy variants are reported in Supplementary Material Section A.

This toy example illustrates that likelihood tempering can have nontrivial and sometimes surprising consequences for optimization performance: by preventing premature overconfidence, it can change the acquisition landscape to steer sampling toward better basins and ultimately yield better outcomes. While this figure is only illustrative, our theory in Section 4 provides a complementary worst-case justification: the regret bounds under tempered posteriors are strictly sharper than their  $\alpha = 1$  counterparts for fixed  $g$ . At the same time, the example also motivates a practical question on how to choose the tempering level  $\alpha$  in a fully sequential BO loop. We defer our discussion on the problem of choosing  $\alpha$  in Section 5 via a prequential, tuning-light schedule motivated by information matching.

### 3 A Linear Surrogate Baseline for Tempered BO

Although our main focus is on Gaussian process (GP) surrogates with nonlinear kernels, we begin with Bayesian linear regression as a more analytically clean baseline. In this finite-dimensional setting, the  $\alpha$ -tempered posterior has a closed form and the effect of tempering can be traced explicitly through both the posterior mean and variance. The resulting regret bound shows that, under correct linear specification, likelihood tempering does not improve or jeopardize the leading-order worst-case guarantee for expected improvement (EI). This “baseline non-improvement” helps isolate where tempering can matter, motivating the GP analysis in Section 4, where kernel mismatch and adaptive localized sampling can induce local overconfidence.

Throughout this section we consider a compact decision set  $\mathcal{X} \subset \mathbb{R}^p$  and a feature map  $\psi : \mathcal{X} \rightarrow \mathbb{R}^d$  satisfying  $\|\psi(x)\|_2 \leq L$  for all  $x \in \mathcal{X}$ . We model the latent reward as linear in the features,  $f(x) = \psi(x)^\top \theta^*$ , where the true parameter  $\theta^* \in \mathbb{R}^d$  is bounded as  $\|\theta^*\|_2 \leq S_\theta$ . Let  $X_t = [\psi(x_1), \dots, \psi(x_t)]^\top \in \mathbb{R}^{t \times d}$  denote the design matrix and  $y_{1:t} = (y_1, \dots, y_t)^\top$  the vector of observations. We place a Gaussian prior  $\theta \sim \mathcal{N}(0, \lambda^{-1} I_d)$  with  $\lambda > 0$  and introduce a tempering parameter  $\alpha \in (0, 1]$ . Since  $y_{1:t} | \theta \sim \mathcal{N}(X_t \theta, \sigma^2 I_t)$  and  $\theta \sim \mathcal{N}(0, \lambda^{-1} I_d)$ , the

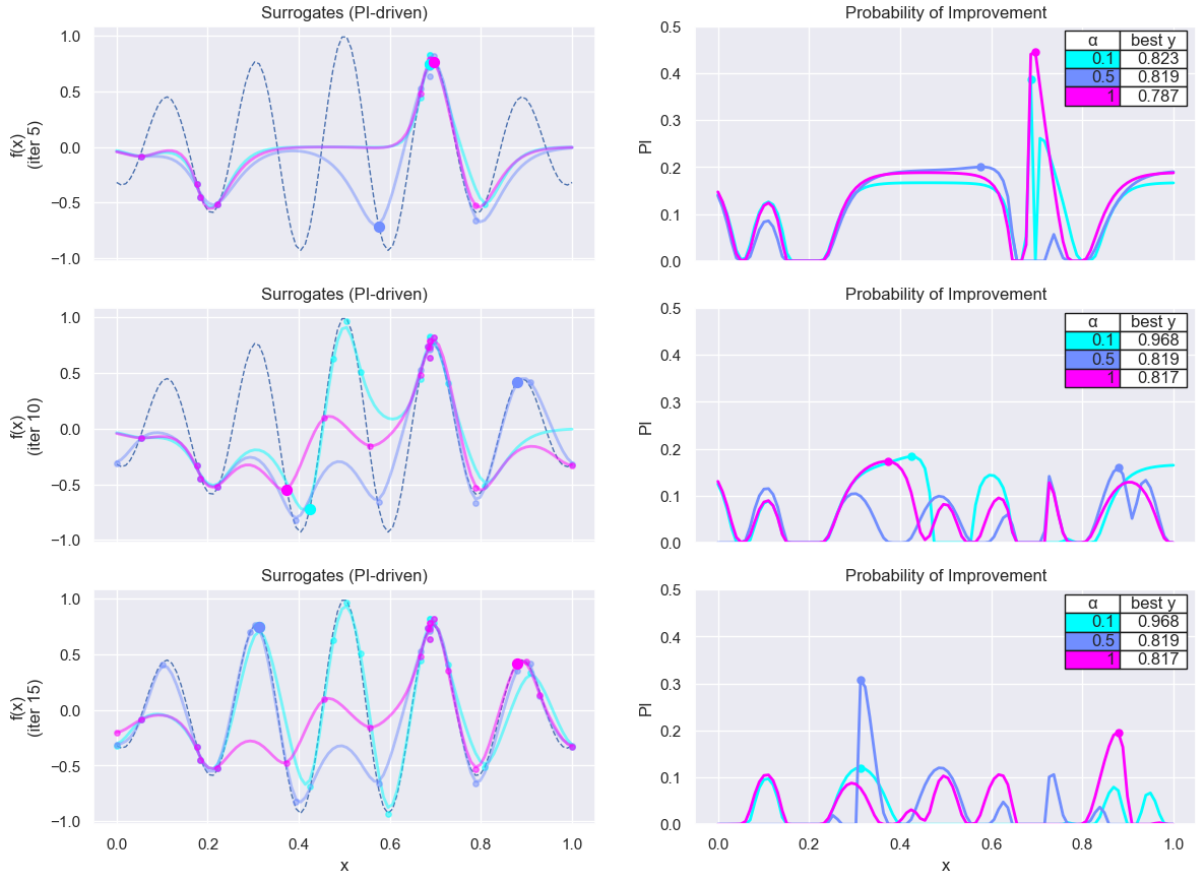


Figure 2: Tempered probability of improvement in one dimension. Each row shows iteration  $t \in \{5, 10, 15\}$ . Left panels plot the true function (3) as a dashed curve and, the posterior mean functions of the surrogates in solid curves for each  $\alpha \in \{0.1, 0.5, 1.0\}$ . Bigger dots are the current candidates, smaller dots are the selected historical candidates. The table reports the best observed value of  $y$  so far for each  $\alpha$ . Right panels plot the probability of improvement curves with their maximizers marked. The surrogate uses a Matérn kernel with  $\nu = 2$  and a white noise term, observations have standard deviation 0.05, five shared random initial points are used at iteration 0.

$\alpha$ -tempered posterior according to (1) is

$$\log p_\alpha(\theta \mid \mathcal{D}_t) = \text{const} - \frac{1}{2} \left[ \lambda \|\theta\|_2^2 + \frac{\alpha}{\sigma^2} \|y_{1:t} - X_t \theta\|_2^2 \right] = \text{const} - \frac{1}{2} \left[ \theta^T V_{t,\alpha} \theta - 2 \theta^T \frac{\alpha}{\sigma^2} X_t^T y_{1:t} \right].$$

Completing the square gives  $\theta \mid \mathcal{D}_t, \alpha \sim \mathcal{N}(\mu_{t,\alpha}, \Sigma_{t,\alpha})$ , where

$$V_{t,\alpha} = \lambda I_d + \frac{\alpha}{\sigma^2} X_t^T X_t, \quad \Sigma_{t,\alpha} = V_{t,\alpha}^{-1}, \quad \mu_{t,\alpha} = \Sigma_{t,\alpha} \frac{\alpha}{\sigma^2} X_t^T y_{1:t}.$$

For any  $x \in \mathcal{X}$  the tempered predictive mean and variance of the latent reward are  $\mu_{t,\alpha}(x; \theta) = \psi(x)^\top \mu_{t,\alpha}$ , and  $\sigma^2 = \sigma_{t,\alpha}^2(x; \theta) = \psi(x)^\top \Sigma_{t,\alpha} \psi(x)$ .

### 3.1 Regret Analysis of Tempered Linear Surrogate

For a maximizer  $x^* \in \arg \max_{x \in \mathcal{X}} f(x)$ , the instantaneous and cumulative regrets are:

$$r_t = f(x^*) - f(x_t), \quad R_T = \sum_{t=1}^T r_t. \quad (4)$$

In the remaining part of Section 3, we focus on expected improvement ( $g = 1$ ) and write  $\mu_{t,\alpha}(x) := \mu_{t,\alpha}(x; \theta)$  and  $\sigma_{t,\alpha}(x) := \sigma_{t,\alpha}(x; \theta)$  for convenience. We assume that

**Assumption 1.** *There exists  $\theta^* \in \mathbb{R}^d$  such that  $f(x) = \psi(x)^\top \theta^*$  for all  $x \in \mathcal{X}$  and  $\|\theta^*\|_2 \leq S_\theta$  for a known constant  $S_\theta > 0$ .*

Write  $m_{t-1} := \mu_{\theta_{t-1},\alpha}^+ = \max_{x \in \mathcal{X}} \mu_{t-1,\alpha}(x; \theta)$  as the running posterior mean maximum. At round  $t$ , the tempered predictive distribution follows  $\mathcal{N}(\mu_{t-1,\alpha}(x), \sigma_{t-1,\alpha}^2(x))$ , and the expected improvement  $\text{EI}_{t-1,\alpha}(x) := \mathbb{E}[(f(x) - m_{t-1})_+ | \mathcal{D}_{t-1}]$  can be written as

$$\text{EI}_{t-1,\alpha}(x) = (\mu_{t-1,\alpha}(x) - m_{t-1}) \Phi(z_{t-1}(x)) + \sigma_{t-1,\alpha}(x) \phi(z_{t-1}(x)), \quad z_{t-1}(x) := \frac{\mu_{t-1,\alpha}(x) - m_{t-1}}{\sigma_{t-1,\alpha}(x)}.$$

The EI policy selects any maximizer  $x_t \in \arg \max_{x \in \mathcal{X}} \text{EI}_{t-1,\alpha}(x)$

Our regret argument uses an *EI-UCB alignment* condition below: it ensures that, over the attainable  $(\mu, \sigma)$  pairs at round  $t$ , the ordering induced by EI is consistent with the linear scalarization  $\mu + \kappa_t \sigma$ . This is a rather strong technical condition (See Remark 8 of [Wang et al. \(2025\)](#)); we impose it only in this warm-up for our intuition and in Section 4 we analyze generalized improvement directly and do not rely on such an alignment assumption.

**Assumption 2.** *There exists  $\kappa_t \geq 0$  such that for all  $x_1, x_2 \in \mathcal{X}$ ,*

$$\mu_{t-1,\alpha}(x_1) + \kappa_t \sigma_{t-1,\alpha}(x_1) \geq \mu_{t-1,\alpha}(x_2) + \kappa_t \sigma_{t-1,\alpha}(x_2) \implies \text{EI}_{t-1,\alpha}(x_1) \geq \text{EI}_{t-1,\alpha}(x_2).$$

**Theorem 3.1** (EI regret bound (fixed  $\alpha$ )). *Suppose Assumption 1-2 holds at each round  $t$  with:*

$$\kappa_t := \beta_{t-1}(\alpha, \delta) = \sqrt{\lambda} S_\theta + \sqrt{\alpha} \sqrt{\log \frac{\det V_{t-1,\alpha}}{\det(\lambda I_d)} + 2 \log \frac{1}{\delta}}.$$

*Then, with probability at least  $1 - \delta$ , for all  $T \geq 1$ ,*

$$R_T \leq 2 \beta_T(\alpha, \delta) \sqrt{c_{\alpha,\lambda} T \cdot \log \frac{\det V_{T,\alpha}}{\det(\lambda I_d)}}, \quad c_{\alpha,\lambda} := \frac{2\sigma^2}{\alpha} + \frac{L^2/\lambda}{\log 2}. \quad (5)$$

The proof of Theorem 3.1 can be found in [Appendix D](#). To control the term  $\log \frac{\det V_{T,\alpha}}{\det(\lambda I_d)}$  in  $R_T$  of (5), we will need the following Lemma.

**Lemma 3.2** (Determinant growth). *For all  $T \geq 1$ ,*

$$\log \frac{\det V_{T,\alpha}}{\det(\lambda I_d)} \leq d \log \left( 1 + \frac{\alpha L^2 T}{\lambda \sigma^2 d} \right).$$

**Corollary 3.3.** *Combining with Lemma 3.2,*

$$R_T \leq 2 \beta_T(\alpha, \delta) \sqrt{c_{\alpha,\lambda} d T \log \left( 1 + \frac{\alpha L^2 T}{\lambda \sigma^2 d} \right)},$$

where

$$\beta_T(\alpha, \delta) = \sqrt{\lambda} S_\theta + \sqrt{\alpha} \sqrt{d \log \left( 1 + \frac{\alpha L^2 T}{\lambda \sigma^2 d} \right) + 2 \log \frac{1}{\delta}}, \quad c_{\alpha,\lambda} = \frac{2\sigma^2}{\alpha} + \frac{L^2/\lambda}{\log 2}.$$

Corollary 3.3 makes the  $\alpha$ -dependence explicit. The factor  $\sqrt{\alpha}$  in  $\beta_T(\alpha, \delta)$  cancels the  $\sqrt{1/\alpha}$  factor in  $c_{\alpha,\lambda}$ , leaving only a slowly varying logarithmic term. On the other hand, The prior component

$$\sqrt{\lambda} S_\theta \sqrt{\left( \frac{2\sigma^2}{\alpha} + \frac{L^2/\lambda}{\log 2} \right) d T \log \left( 1 + \frac{\alpha L^2 T}{\lambda \sigma^2 d} \right)}$$

typically favors larger  $\alpha$  (closer to 1), up to logarithmic factors. Thus, in the correctly specified linear model and under Assumption 1-2, tempering is not expected to improve worst-case cumulative regret for EI, and may slightly worsen constants.

This negative result is informative rather than discouraging: it suggests that any theoretical or empirical gains from tempering should be attributed to settings where the surrogate can become locally overconfident under adaptive design, a phenomenon that is substantially more plausible for nonlinear GP kernels. We turn to this regime in Section 4, where we analyze tempered GP surrogates and generalized improvement acquisitions without requiring an EI-UCB alignment condition. We move beyond this linear parametric kernel to Matérn and squared-exponential kernels, where the induced feature map is effectively infinite-dimensional and the interaction between acquisition-level choices and surrogate-level tempering, becomes nontrivial.

## 4 Bayesian GP Surrogates

In practice, the predominant approach in BO is to start by fitting a standard GP regression on the current data collection  $x_{1:t}$  and use it as a surrogate for the unknown function  $f$  (Gramacy, 2020):

$$f(x_{1:t})|\theta \sim \mathcal{N}(m(x_{1:t}), K^\theta(x_{1:t}, x_{1:t})),$$

where  $m(\cdot)$  is the mean function, and  $\theta$  parameterizes the covariance function  $K^\theta(x_{1:t}, x_{1:t}) = k^\theta(x_i, x_j)$ . Without loss of generality, we consider a zero-mean function prior, and the covariance kernel is parametrized by  $d$  length-scale hyperparameter  $\theta$  estimated by maximum likelihood estimates (MLE). We will focus on squared exponential (Matern- $\infty$ ) unless otherwise is stated:  $k_{\text{SE}}^\theta(\mathbf{x}, \mathbf{x}') = \exp(-\frac{1}{2}r^2)$  where  $r^2 = (\mathbf{x} - \mathbf{x}')^\top \text{diag}(\theta^2)^{-1}(\mathbf{x} - \mathbf{x}')$ .

## 4.1 Tempered Posteriors

Consider the case where we update the GP surrogate model using the  $\alpha$ -posterior with  $\alpha > 0$ . After  $t$  steps with dataset  $\mathcal{D}_t = \{(x_s, y_s)\}_{s=1}^t$ , we define  $x_{1:t} := [x_1, \dots, x_t]$ ,  $y_{1:t} := [y_1, \dots, y_t]$ ,  $K_t := [k(x, x')]_{x, x' \in x_{1:t}}$  we have the  $\alpha$ -posterior in (1) on the vector  $f := [f(x_1), \dots, f(x_t)]$ :

$$\begin{aligned} p_\alpha(f | \mathcal{D}_t) &\propto p(f)(p(y_{1:t} | f))^\alpha \\ &\propto \exp\left\{-\frac{1}{2}f^T(K_t)^{-1}f\right\} \exp\left\{-\frac{1}{2}(y_{1:t} - f)^T\left(\frac{\sigma^2}{\alpha}\mathbb{I}\right)^{-1}(y_{1:t} - f)\right\} \\ &\sim N(\mu_{t,\alpha}, \Sigma_{t,\alpha}), \end{aligned}$$

where  $\mu_{t,\alpha} = K_t \left(K_t + \frac{\sigma^2}{\alpha}\mathbb{I}\right)^{-1} y_{1:t}$ ,  $\Sigma_{t,\alpha} = K_t - K_t \left(K_t + \frac{\sigma^2}{\alpha}\mathbb{I}\right)^{-1} K_t$ . To evaluate an arbitrary point  $x \in \mathcal{X}$  using the updated surrogate model, we define  $k_t(x) = [k(x_1, x), \dots, k(x_t, x)]^T$ , and obtain

$$\begin{aligned} \mu_{t,\alpha}(x; \theta) &= k_t(x)^T \left(K_t + \frac{\sigma^2}{\alpha}\mathbb{I}\right)^{-1} y_{1:t}, \\ k_{t,\alpha}(x, x') &= k(x, x') - k_t(x)^T \left(K_t + \frac{\sigma^2}{\alpha}\mathbb{I}\right)^{-1} k_t(x'), \\ \sigma_{t,\alpha}^2(x; \theta) &= k_{t,\alpha}(x, x). \end{aligned}$$

## 4.2 The $g$ -EI Acquisition Function

Our regret analysis covers the entire  $g$ -EI family for  $g \geq 0$ , which includes both probability of improvement ( $g = 0$ ) and classical expected improvement ( $g = 1$ ). Under the  $\alpha$ -tempered GP posterior, the latent objective at any fixed  $x$  has the predictive distribution  $f(x) | \mathcal{D}_t, \alpha, \theta \sim \mathcal{N}(\mu_{t,\alpha}(x; \theta), \sigma_{t,\alpha}^2(x; \theta))$ , and we measure improvement relative to the current posterior-mean maximizer  $\mu_{\theta_t, \alpha}^+(x; \theta) = \max_{x \in \mathcal{X}} \mu_{t,\alpha}(x; \theta)$ . The following proposition shows the  $g$ -EI family defined in (2) has a convenient analytical expression:

**Proposition 4.1.** *For  $\alpha \in (0, 1]$  and  $g \geq 0$ , Let  $v_\alpha = \frac{\mu_{\theta_t, \alpha}^+ - \mu_{t,\alpha}(x; \theta)}{\sigma_{t,\alpha}(x; \theta)}$  and  $T_m(v) :=$*

$\int_v^\infty u^m \phi(u) du$ . Then the  $g$ -EI family defined in (2) can be rewritten as:

$$\alpha_{\theta,g,\alpha}^{\text{EI}(f)}(x \mid \mathcal{D}_t) = \sigma_{t,\alpha}^g(x; \theta) \tau_g(v_\alpha), \quad \tau_g(v) := \int_v^\infty (u - v)^g \phi(u) du. \quad (6)$$

If  $g \in \mathbb{N}_{\geq 0}$ ,  $\tau_g(\cdot)$  can be further simplified and:

$$\alpha_{\theta,g,\alpha}^{\text{EI}(f)}(x \mid \mathcal{D}_t) = \sigma_{t,\alpha}^g(x; \theta) \sum_{k=0}^g (-1)^k \binom{g}{k} v_\alpha^k T_{g-k}(v_\alpha),$$

where  $T_0(v) = \Phi(-v)$ ,  $T_1(v) = \phi(v)$ , and for  $m > 1$ ,  $T_m(v) = v^{m-1} \phi(v) + (m-1)T_{m-2}(v)$ .

Following Wang and de Freitas (2014), we introduce a positive rescaling parameter  $\nu_{\theta_t}$  that modulates the exploration level by inflating the posterior standard deviation inside the acquisition. In the noise-free GP setting,  $\nu_{\theta_t}^2$  leaves the posterior mean unchanged and scales the posterior standard deviation by  $\nu_{\theta_t}$ . Our regret bounds require mild growth conditions on  $\nu_{\theta_t}$ , analogous to those in Theorem 1 of Wang and de Freitas (2014). Our bounds echo the Wang et al. (2025) and Wang and de Freitas (2014) for  $\alpha = 1$ , and the technique can be extended to Matern- $\nu$  kernels as shown by Wang et al. (2025); and our analysis here is more general for a wider family of acquisition functions and  $\alpha \in (0, 1]$ .

Combining  $\nu_t$  with proposition 4.1, we work with the rescaled version of the acquisition function:

$$\alpha_{\theta,g,\alpha}^{\text{EI}(f)}(x \mid \mathcal{D}_t) = \nu_{\theta_t}^g \sigma_{t,\alpha}^g(x; \theta) \tau_g\left(\frac{v_\alpha}{\nu_{\theta_t}}\right), \quad (7)$$

with  $v_\alpha = \frac{\mu_{\theta_t,\alpha}^+ - \mu_{t,\alpha}(x; \theta)}{\sigma_{t,\alpha}(x; \theta)}$  and the function  $\tau_g(\cdot)$  defined in (6). Note by Proposition 4.1, the integer  $g$  case has a much simpler expressions.

### 4.3 Regret Analysis of Tempered GP Surrogate

To derive the regret bound of our proposed acquisition function, we have to adopt the  $\alpha$ -posterior version of the *maximum mutual information gain* at step  $t = 1, \dots, T$  defined as follows:

$$\gamma_{t,\alpha}^\theta = \max_{A \subset \mathcal{X}: |A|=t} \frac{1}{2} \log |\mathbb{I} + \alpha \sigma^{-2} \mathbf{K}_A^\theta|,$$

where  $\mathbf{K}_A^\theta$  is the covariance kernel matrix on subset of  $A \subset \mathcal{X}$ . When  $\alpha = 1$  in the standard GP setting, the  $\gamma_{T,1}$  term frequently appeared in the BO regret analysis literature (Garnett, 2023; Srinivas et al., 2012). Without loss of generality, we assume the prior variance  $k(x, x) = 1$  and present the following cumulative regret bound under general choices of  $g \geq 1$  and  $\alpha$ , with proof presented in Appendix F:

**Theorem 4.2.** For any  $g \geq 1$  and  $\alpha \in (0, 1]$ , let  $C_{(g)} := \frac{2^{g/2} \Gamma((g+1)/2)}{2\sqrt{\pi}}$  and for a fixed  $\delta > 0$ ,

define

$$m_{\alpha,t}^\theta := \sqrt{\alpha} \left( \sqrt{\gamma_{t-1,\alpha}^{\theta_t}} + \sqrt{\log \frac{2t^2\pi^2}{3\delta}} \right),$$

If  $\nu_{\theta_t}$  is the same order of  $m_{\alpha,t}$  such that  $|\frac{m_{\alpha,t}}{\nu_{\theta_t}}| \leq C_1$  for some constant  $C_1 > 0$ , and  $\theta^L \leq \theta_t \leq \theta^U$  for all  $t \geq 1$  such that  $C_2 := \prod_{i=1}^d \frac{\theta_i^U}{\theta_i^L}$ , then with probability at least  $1 - \delta$ , the cumulative regret obeys the following rate:

$$R_T = \mathcal{O} \left( \beta_{T,\alpha,g} \sqrt{\gamma_{T,\alpha}^{\theta_L} T / \alpha} \right),$$

where

$$\beta_{T,\alpha,g} = \sqrt{2C_2} \|f\|_{\mathcal{H}_{\theta^U}} + \left[ C_1 C_3 C_{(g)}^{1/g} + 2\sqrt{2} + C_1 \tau_g^{-1} \left( C_{(g)} \left( \frac{\sigma^2}{\alpha(T-1) + \sigma^2} \right)^{g/2} \right) \right] m_{\alpha,T}^{\theta_L}.$$

and the function  $\tau_g^{-1}(\cdot)$  is the well-defined inverse function of  $\tau_g(\cdot)$  in equation (6).

Theorem 4.2 favors smaller choice of  $\alpha$  over the standard choice of  $\alpha = 1$ . To see this more transparently, it is convenient to rewrite the regret bound as  $\frac{\beta_{T,\alpha,g}}{\sqrt{\alpha}} \sqrt{\gamma_{T,\alpha}^{\theta_L} T}$ . The maximum information gain  $\gamma_{T,\alpha}$  is increasing and concave in  $\alpha$ . By Lemma F.2 in the Appendix, the function  $\tau_g(\cdot)$  is strictly decreasing and thus its inverse function  $\tau_g^{-1}(\cdot)$  is also a decreasing function by the inverse derivative formula. It follows that  $\beta_{T,\alpha,g}$  is increasing in  $\alpha$ , since  $m_{\alpha,T}^{\theta_L}$  is increasing in  $\alpha$ , and  $\tau_g^{-1}(\cdot)$  is a decreasing function and hence an increasing function in  $\alpha$  as well. After divide  $\beta_{T,\alpha,g}$  by a  $\sqrt{\alpha}$  factor, the  $\sqrt{\alpha}$  factor in  $m_{\alpha,T}^{\theta_L}$  is canceled, leaving an expression whose dominant terms are increasing functions of  $\alpha$ . Therefore, for large horizon  $T$ , Theorem 4.2 suggests that moderately tempering the posterior yields strictly smaller worst-case regret guarantee than the standard Bayesian posterior ( $\alpha = 1$ ). Next, we consider the setting where  $0 \leq g < 1$ .

**Theorem 4.3.** Consider the same setup and assumptions as in Theorem 4.2. Let  $0 \leq g < 1$  and define  $\eta_{\alpha,g,T} := C'_g (m_{\alpha,t,\theta_L})^g \left( \frac{\sigma^2}{\alpha(T-1) + \sigma^2} \right)^{(g-1)/2}$ , where  $C'_g > 0$  is a constant depending only on  $g$ . Then, with probability at least  $(1 - \delta)$ ,

$$R_T = \mathcal{O} \left( \beta_{T,\alpha,g} \sqrt{\gamma_{T,\alpha}^{\theta_L} T / \alpha} \right),$$

where

$$\beta_{T,\alpha,g} = \sqrt{2C_2} \|f\|_{\mathcal{H}_{\theta^U}} + \left[ 2\sqrt{2} + C_1 \tau_g^{-1} \left( C_{(g)} \left( \frac{\sigma^2}{\alpha(T-1) + \sigma^2} \right)^{g/2} \right) \right] m_{\alpha,t}^{\theta_L} + \eta_{\alpha,g,T}.$$

Theorem 4.3 suggests that the same beneficial effects of tempering on the worst case

regret continues to hold for  $0 \leq g < 1$ . The regret bound looks similar to the  $g \geq 1$  case, but includes an extra factor of  $\eta_{\alpha,g,T}$ . When analyzing  $\frac{\beta_{T,\alpha,g}}{\sqrt{\alpha}}$ , we note tempering does not play major effects in  $\frac{\eta_{\alpha,g,T}}{\sqrt{\alpha}}$  since the leading  $\alpha$  term is canceled out. Therefore, the same reasoning applies and tempering continues to yield a uniformly smaller leading constant in the regret bound for  $0 \leq g < 1$ .

Beyond the effect of tempering, Theorems 4.2-4.3 also clarify how the choice of  $g$  can influence the upper regret bounds. For  $g \geq 1$ , the term  $C_{(g)}^{1/g}$  in Theorem 4.2 is weakly increasing in  $g$  and, as shown in Remark 4.4, the function  $\tau_g^{-1}(\cdot)$  grows on the order of  $\Theta(\sqrt{g \log T})$ . It follows that taking  $g > 1$  cannot improve the asymptotic rate and can only enlarge the constant. In contrast, for  $0 \leq g < 1$ , Theorem 4.3 contains the additional term  $\eta_{\alpha,g,T}$ , which yields an extra  $T^{(1-g)/2}$  factor in the cumulative regret, strictly worsening the regret bound for  $g \geq 1$  case. In particular, the extreme  $g = 0$  case suffers the worst theoretical rate in the  $g$ -EI family. This aligns with the well-known intuition that PI is overly exploitative since it ignores the magnitude of the improvement, which consequently makes the cumulative regret harder to control (Garnett, 2023).

To summarize, Theorems 4.2 and 4.3 illustrate that, for any fixed  $g$  in the  $g$ -EI family, tempering with  $\alpha < 1$  is universally helpful in our cumulative regret bound. Additionally, lowering  $g$  below 1 is asymptotically harmful, while extra exploration with  $g > 1$  does not improve the rate and can only worsen the constants. These results provide a theoretical rationale for the empirical success of the standard expected improvement rule ( $g = 1$ ). At the same time, it should be acknowledged that our guarantees are upper bounds on cumulative regrets, and the analysis is solely derived based on the popular  $g$ -EI family. In particular, they do not capture all aspects of empirical behavior: as shown in the experiments in Section 6, tempering appears to be much more beneficial to probability of improvement (smaller  $g$ ) than to expected improvement (larger  $g$ ). This is intuitively reasonable, but our theorems are not sharp enough to reflect this empirical observation (See Appendix H). We conclude this section by comparing our regret bounds to existing results in the BO literature.

**Remark 4.4.** *Based on Theorem 4.2, our regret bound for the expected improvement acquisition function with standard posterior  $\alpha = 1$  is strictly tighter by a factor  $(\log T)^{1/2}$  than the existing BO literature for expected improvement (Wang and de Freitas, 2014), which suggests  $\beta_T^{(\text{lit})} = \Theta(\log T \gamma_{T-1}^{\theta_L})$ . In contrast, our regret bound is of the order  $\beta_{T,1,1} = \Theta(\sqrt{\log T} \gamma_{T-1}^{\theta_L})$ . To see this, recall  $\tau_1(z) = \phi(z) - z\Phi(z)$ . By Mills' ratio, for  $z \rightarrow \infty$ , we have*

$$\tau_1(z) = \phi(z) - z(1 - \Phi(z)) = \frac{\phi(z)}{z^2} (1 + O(z^{-2})).$$

Set  $y = \frac{1}{\sqrt{2\pi}} \sqrt{\frac{\sigma^2}{(T-1)+\sigma^2}} = \Theta(T^{-1/2})$ . Solving  $y \asymp \frac{1}{\sqrt{2\pi}} \frac{e^{-z^2/2}}{z^2}$  gives

$$\tau_1^{-1}(y) = \Theta(\sqrt{\log T}).$$

More generally, using the integral form  $\tau_g(z) = \int_0^\infty t^g \phi(z+t) dt = \phi(z) \int_0^\infty t^g e^{-zt - \frac{1}{2}t^2} dt$  and a Laplace approximation as  $z \rightarrow \infty$ , we obtain  $\tau_g(z) = \frac{\Gamma(g+1)}{\sqrt{2\pi}} \frac{e^{-z^2/2}}{z^{g+1}} (1+O(z^{-2}))$ . Let  $y_T = C_{(g)} r^{g/2}$  and  $r = \frac{\sigma^2}{\alpha(T-1) + \sigma^2}$ , and set  $-\log y_T = -\log C_{(g)} - \frac{g}{2} \log r = -\log C_{(g)} + \frac{g}{2} \log\left(\frac{\alpha(T-1)+\sigma^2}{\sigma^2}\right)$ . Inverting the asymptotic yields

$$\tau_g^{-1}(C_{(g)} r^{g/2}) = \Theta\left(\sqrt{g \log\left(\frac{\alpha(T-1)+\sigma^2}{\sigma^2}\right)}\right) = \Theta(\sqrt{g \log T}).$$

## 5 Tempering Schedule Design

Our regret bounds in Section 4 show that, for any fixed acquisition parameter  $g$ , tempering the GP posterior ( $\alpha < 1$ ) yields strictly sharper worst-case guarantees than using the standard posterior ( $\alpha = 1$ ). In practice, when researchers have access to a large external dataset  $\mathcal{D}_n$ , existing methods may be used to estimate an appropriate tempering level  $\hat{\alpha}$  (e.g., [Holmes and Walker \(2017\)](#); [Miller and Dunson \(2019\)](#)), see [Wu and Martin \(2023\)](#) for a comprehensive review of how to choose  $\alpha$ . However, in many Bayesian optimization settings, such calibration dataset is unavailable, and picking the “optimal”  $\alpha$  remains challenging. We hence develop an adaptive strategy for choosing  $\alpha$  based on information-matching principle: the tempering level is chosen so that the prior expected information gain from a single observation under a possibly misspecified model matches the gain one would obtain if the model were correct. Our idea of designing a tempering schedule follows [Holmes and Walker \(2017\)](#), who propose to choose  $\alpha$  such that

$$\alpha = \left\{ \frac{\int f(x; \theta_0) \Delta(x) dx}{\int f_0(x) \Delta(x) dx} \right\}^{\frac{1}{2}}, \quad (8)$$

where  $f_0(x)$  is the true data density,  $f(x; \theta_0)$  is the pseudo true model that minimizes the KL divergence to  $f_0(x)$ , and  $\Delta(x)$  is the Fisher-divergence information between a posterior update from its prior, with likelihood  $f(x; \theta)$ . Our adaptation of this principle leads to a simple, tuning-free, and computationally efficient procedure for choosing  $\alpha$  online.

Fix a design point  $x \in \mathcal{X}$  and write the local parameter of interest as  $\theta = f(x)$ , under the working observation model, we have  $y|\theta \sim \mathcal{N}(\theta, \sigma^2)$ . Following [Holmes and Walker](#)

(2017), we quantify the information of a single update at  $x$  as

$$\begin{aligned}\Delta_t(x; y) &:= \mathbb{E}_{\theta \sim N(\mu_{t-1,1}(x), \sigma_{t-1,1}^2(x))} \left[ \left( \frac{\partial}{\partial \theta} \log p(y|\theta) \right)^2 \right] \\ &= \mathbb{E} \left[ \left( \frac{(y - \theta)}{\sigma^2} \right)^2 \right] = \frac{(y - \mu_{t-1,1}(x))^2 + \sigma_{t-1,1}^2(x)}{\sigma^4}.\end{aligned}$$

Note that we have used  $(\mu_{t-1,1}(x), \sigma_{t-1,1}^2(x))$  to denote the regular untempered GP predictive mean and variance given  $\mathcal{D}_{t-1}$ . Under a likelihood power  $\alpha$ , the score is multiplied by  $\alpha$  and the squared score by  $\alpha^2$ . Consequently, the one-step information measure under tempering is  $\Delta_{t,\alpha}(x; y) = \alpha^2 \Delta_t(x; y)$ .

We now take expectations of  $\Delta_t(x; y)$  with respect to two different distributions for  $y|x$ . When our GP model is correctly specified, we have  $y|x \sim N(\theta_0(x), \sigma^2)$ , where  $\theta_0(x)$  represents the true signal value at  $x$ . It follows

$$\mathbb{E}_{\text{model}}[\Delta_t(x; Y) | x] = \frac{\sigma_{t-1,1}^2(x) + \sigma^2 + (\theta_0(x) - \mu_{t-1,1}(x))^2}{\sigma^4}.$$

When our model is misspecified, we let  $y|x \sim f_0(\cdot|x)$  with mean  $m_0(x)$ , variance  $v_0(x)$ . Then we have

$$\mathbb{E}_0[\Delta_t(x; Y) | x] = \frac{\sigma_{t-1,1}^2(x) + v_0(x) + (m_0(x) - \mu_{t-1,1}(x))^2}{\sigma^4} = \frac{\sigma_{t-1,1}^2(x) + \text{MSE}_t(x)}{\sigma^4},$$

where  $\text{MSE}_t(x) := \mathbb{E}_0[(Y - \mu_{t-1,1}(x))^2 | x]$ .

Following Holmes and Walker (2017), we choose a local tempering level  $\alpha_t(x)$  so that the tempered information under the true world matches the information under the as-if-correct model world so that  $\alpha_t(x)^2 \mathbb{E}_0[\Delta_t(x; Y) | x] = \mathbb{E}_{\text{model}}[\Delta_t(x; Y) | x]$ . Therefore,

$$\alpha_t^2(x) = \frac{\mathbb{E}_{\text{model}}[\Delta_t(x; Y) | x]}{\mathbb{E}_0[\Delta_t(x; Y) | x]} = \frac{\sigma_{t-1,1}^2(x) + \sigma^2 + (\theta_0(x) - \mu_{t-1,1}(x))^2}{\sigma_{t-1,1}^2(x) + v_0(x) + (m_0(x) - \mu_{t-1,1}(x))^2}. \quad (9)$$

Under correct specification,  $(m_0(x), v_0(x)) = (\theta_0(x), \sigma^2)$ , and (9) gives  $\alpha_t(x) = 1$ .

For implementation, it is impractical to specify different  $\alpha$  values at each  $x$  and we need to aggregate across visited points  $x_t$  and use prequential quantities in the schedule. Although  $(m_0(x), v_0(x))$  is unknown, observe that by the standard bias-variance trade-off formula,  $\text{MSE}(x) := \mathbb{E}[(y - \mu_{t-1,1}(x))^2 | x] = v_0(x) + (m_0(x) - \mu_{t-1,1}(x))^2$ . Based on  $\mathcal{D}_t$ , we may compute a prequential estimator of the global tempering weight at time  $t$  is

$$\widehat{\alpha}_t = \min \left\{ \sqrt{\frac{\frac{1}{t} \sum_{s=1}^t \{\sigma_{s-1,1}^2(x_s) + \widehat{\sigma}^2\}}{\frac{1}{t} \sum_{s=1}^t \{\sigma_{s-1,1}^2(x_s) + \widehat{\text{MSE}}_s\}}}, 1 \right\}, \quad \widehat{\text{MSE}}_s := (y_s - \mu_{s-1,1}(x_s))^2, \quad (10)$$

where  $\hat{\sigma}^2$  denotes a global estimate of the observation-noise variance. This estimator depends only on prequential quantities  $(\mu_{s-1,1}(x_s), \sigma_{s-1,1}^2(x_s))$  and adopts a conservative information-matching approximation by setting the model-side bias term  $(\theta_0(x_s) - \mu_{t-1,1}(x_s))^2$  to zero in the as-if-correct world. In practice, (10) is easy to compute and typically yields  $\hat{\alpha}_T \leq 1$  early in BO, since  $\widehat{\text{MSE}}_t$  reflects both noise and misspecification; as posterior uncertainty contracts under correct specification and with consistent  $\hat{\sigma}^2$ , the ratio drifts toward 1. We present our entire BO framework with scheduled tempered posterior in Algorithm 2 of Appendix E.

Our proposed tempering schedule in (10) is highly general and remains coherent even when applied to acquisition functions beyond the  $g$ -EI family. We conclude this section with Proposition 5.1, which establishes that the proposed tempering schedule is well-behaved asymptotically. In the well-specified regime, the schedule satisfies  $\hat{\alpha}_t$  approaching to 1 asymptotically, indicating no tempering is needed. In contrast, when the model is misspecified, we have  $\hat{\alpha}_t$  converges to a limit smaller than 1, reflecting the reduced information that each observation contributes relative to the misspecified surrogate.

**Proposition 5.1** (Limits of the Adaptive Schedule). *Let  $\{\mathcal{F}_s\}_{s \geq 0}$  be the filtration generated by BO history, and assume  $y_s = f(x_s) + \varepsilon_s$  with  $\mathbb{E}[\varepsilon_s | \mathcal{F}_{t-1}] = 0$ ,  $\mathbb{E}[\varepsilon_s^2 | \mathcal{F}_{s-1}] = \sigma^2 > 0$ . Define  $\text{PV}_t := \frac{1}{t} \sum_{s=1}^t \sigma_{s-1,1}^2(x_s)$ ,  $\text{MSE}_t := \frac{1}{t} \sum_{s=1}^t (y_s - \mu_{s-1,1}(x_s))^2$ , and  $e_s := \mu_{t-1,1}(x_s) - f(x_s)$ . Assume that  $\sup_t |e_t| < \infty$  a.s. Then*

- i) *Well-specified: if  $\frac{1}{t} \sum_{s=1}^t e_s^2 \xrightarrow{p} 0$ , then  $\hat{\alpha}_t \xrightarrow{p} 1$ .*
- ii) *Misspecified: if  $\frac{1}{t} \sum_{s=1}^t e_s^2 \xrightarrow{p} b^2$  for some  $0 < b^2 < \infty$ . Then  $\hat{\alpha}_t \xrightarrow{p} \sqrt{\frac{\text{PV}_\infty + \sigma^2}{\text{PV}_\infty + \sigma^2 + b^2}} < 1$ .*

## 6 Experiments

### 6.1 Simulation study on benchmark optimization functions

We evaluate the effects of  $\alpha$  and  $g$  on a suite of challenging benchmark optimization functions (Surjanovic and Bingham). The function suite contains 47 distinct functions exhibiting multiple local minima and diverse geometries. For functions without a fixed intrinsic dimension, we consider dimension  $p \in \{5, 10\}$ ; functions with a native dimension are used as is. This yields 61 distinct function-dimension instances in total.

For each of the 61 functional forms, we run 5 independent Bayesian optimization trials (different random seeds) for every configuration of  $(\alpha, g)$ , with  $\alpha \in \{1, \text{Tempered}\}$  and  $g \in \{0, 1, 2\}$ . The GP posterior is adaptively tempered as described in Section 5. In total, we perform  $61 \times 5 \times 2 \times 3 = 1,830$  experiments. For a  $p$ -dimensional objective function, we randomly initialized with a data set with size  $\min\{5, 2p\}$ , and conducted  $\min\{30, 10p\}$  iterations of optimization. We allow for different iteration budgets because

Table 1: Paired comparison of  $\alpha \in \{1, \text{hw}\}$  across 61 functions (seed-averaged) for each  $g$ . Lower *Avg. rank* is better; *Avg. margin to best* closer to 0 (less negative) is better.  $p$ -values from Wilcoxon signed-rank (one-sided,  $H_1$ : the median of the paired difference is larger than 0 (tempering is better)).

$\alpha$	Wins	Strict win rate	Avg. rank $\downarrow$	Avg. margin to best $\uparrow$	Avg. norm margin $\uparrow$
PANEL A: $g = 0$					Wilcoxon paired $p = 0.041$
1.0	23	37.7%	1.63	-30.86	-0.63
Tempered	38	62.3%	1.37	-2.95	-0.37
PANEL B: $g = 1$					Wilcoxon paired $p = 0.097$
1.0	28	45.9%	1.55	-24.25	-0.54
Tempered	33	54.1%	1.46	-11.18	-0.44
PANEL C: $g = 2$					Wilcoxon paired $p = 0.932$
1.0	39	63.9%	1.37	-6.33	-0.36
Tempered	22	36.1%	1.63	-12.12	-0.62

Notes: Avg margin to best is  $\frac{1}{|F|} \sum_{f \in F} (y_{f,a} - \max_{a'} y_{f,a'})$  (thus  $\leq 0$  and larger is better). Avg normalized margin (range) uses range normalization:  $\frac{1}{|F|} \sum_f \frac{y_{f,a} - \max_{a'} y_{f,a'}}{\max_{a'} y_{f,a'} - \min_{a'} y_{f,a'} + \varepsilon} \in [-1, 0]$ .

when the dimension is small, allowing substantially more evaluations tends to diminish meaningful differences among BO strategies, as most methods eventually identify the global optimum. The observational noise  $\sigma$  is set to be 0.01.

Table 1 summarizes the comparative performance of  $\alpha \in \{1, \text{Tempered}\}$  across 61 benchmark functions (each seed-averaged) for fixed values of  $g$ . For each  $g$ , we report the number of functions won in terms of averaged observed values, the strict win rate, and several aggregated performance statistics across functions: this includes the average rank (lower is better) and the raw average margin to the best outcome of a given function defined in the table. Since the raw margin is scale-dependent, we also compute the normalized average margin (bounded in  $[-1, 0]$ ) for more robust comparison. All results are paired by function, and the reported  $p$ -values are from the Wilcoxon signed-rank test, which tests whether the median paired improvement of tempering over  $\alpha = 1$  exceeds zero.

For  $g = 0$ , our adaptive tempering approach yields a substantial and statistically significant improvement ( $p = 0.041$ ): the tempered posterior wins 38 out of 61 cases, achieves a lower average rank, and exhibits much smaller raw and absolute margins. This behavior not only echos our discussion of Theorem 4.2, but also aligns with our theoretical intuition: as probability of improvement is known to be overly exploitative (Garnett, 2023), tempering the posterior effectively encourages additional principled exploration and tends to yields better optimization results.

Tempering also offers a modest advantage for the  $g = 1$  expected improvement setting, leading to higher win rates and better average ranks. Although the effect is only marginally

Table 2: Aggregate outcomes by  $g$  (seed-averaged within function; aggregated across 61 functions). Conditional regular posterior case ( $\alpha = 1$ )

$g$	Strict wins	Strict win rate	Avg. rank ↓	Avg. margin to best ↑	Avg. norm margin to best ↑
0	25	0.41	2.10	-46.30	-0.54
1	22	0.36	1.84	-48.51	-0.42
2	14	0.23	2.07	-43.65	-0.48

Notes: Avg margin and Avg norm. margin are defined in Table 1.

significant in our experimentation ( $p = 0.097$ ), both the raw and normalized margin metrics are more stable under the tempered posterior. This indicates that in instances where the regular posterior outperforms tempering, its advantage tends to be relatively small compared to the cases where tempering wins.

Notably, tempering the posterior significantly deteriorates the situation where  $g = 2$  based on Panel C of Table 1. A plausible explanation is that  $g = 2$  already promotes aggressive exploration, and tempering further inflates posterior uncertainty, inducing excessive exploration and thus degrading finite-sample performance. The overly exploration behavior can also lead to larger MSE, which induces stronger tempering effect of  $\alpha$  based on the estimator in equation (10).

Table 2 compares the performance across different choices of  $g$  when using the standard posterior ( $\alpha = 1$ ). The results show that moderate values of  $g$  (i.e.,  $g = 0$  or  $g = 1$ ) lead to overall better optimization performance compared with  $g = 2$  in terms of strict win rates. The inferior performance of  $g = 2$  provides empirical support for our theoretical regret bound: larger  $g$  overemphasizes exploration, which increases the regret upper bound and slows practical convergence. In contrast, smaller  $g$  values strike a more balanced exploration behavior under the regular posterior.

To conclude this section, we visualize the progression of median regret and interquartile range over iterations for two posterior configurations across three representative test functions and two acquisition settings ( $g = 0, 1$ ) in Figure 3. Across these settings, tempering consistently accelerates regret minimization for the more exploitative  $g = 0$  configuration and often provides moderate gains for  $g = 1$ , where exploration is already stronger (See Appendix I). However, we would like to highlight that tempering does not guarantee improvements on every function and design, but it is generally favorable in performance.

## 6.2 Real data: materials optimization

We use the *Fe–Ga–Pd* materials-optimization dataset originally introduced by [Long et al. \(2007\)](#) and later adopted in the Bayesian active learning literature ([Kusne et al., 2020](#)). Each sample corresponds to a ternary alloy characterized by its composition fractions of

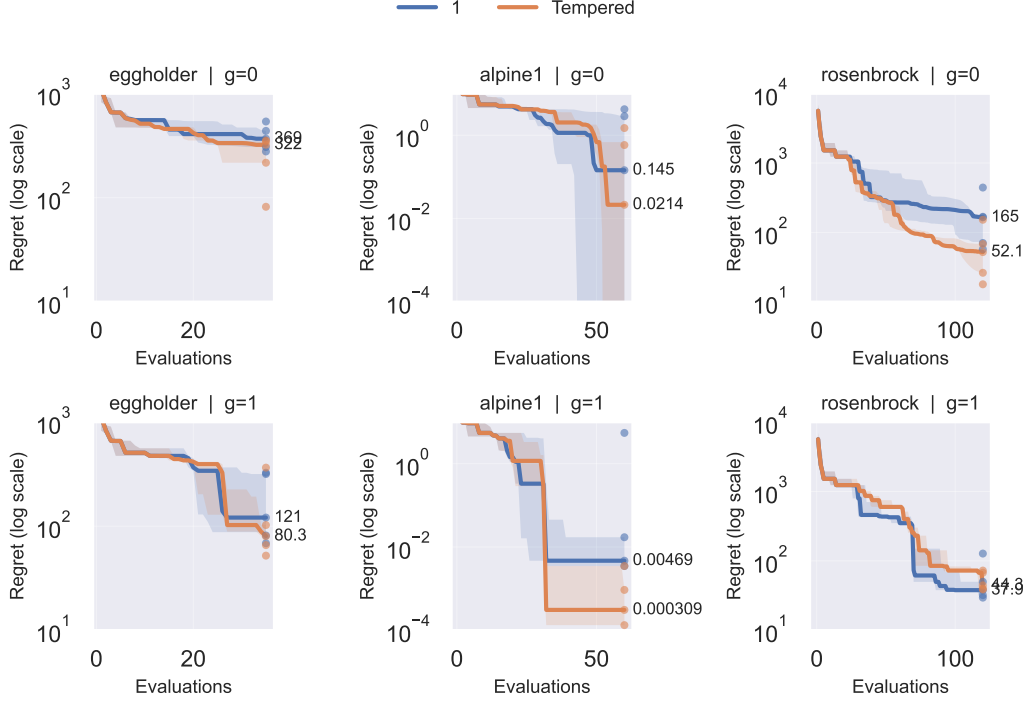


Figure 3: Effects of Tempering on Selected benchmarks: iterations v.s. log-regret

*Notes.* Ribbons are the 25–75% interquartile range across seeds at each iteration. The dots at the right edge represent the log regret for a single BO trial, and the numbers annotate the terminal *median* regret across all trials. Note that for a  $p$ -dimensional function, we conducted  $\min\{30, 10p\}$  evaluations.

iron (Fe), gallium (Ga), and palladium (Pd), which together satisfy the simplex constraint  $\text{Fe} + \text{Ga} + \text{Pd} = 1$ ,  $\text{Fe}, \text{Ga}, \text{Pd} \geq 0$ . The response variable is the *remanent magnetization*, measured as the output voltage of a scanning SQUID (Superconducting Quantum Interference Device) microscope (Long et al., 2007). Our objective is to identify the alloy composition that maximizes the SQUID voltage, corresponding to the highest remanent magnetization. Compositions with strong magnetic responses are of interest for applications in actuators and sensors. Because experimental evaluation of new compositions is both costly and time-consuming, Bayesian optimization provides a natural and efficient framework for this search.

Given the simplex constraint, we reparameterize the domain in two dimensions by  $(\text{Fe}, \text{Ga})$ , with  $\text{Pd} = 1 - \text{Fe} - \text{Ga}$ . For offline benchmarking, we fit a GP model with a Matérn-5/2 kernel to all 278 available measurements and treat its posterior mean function as the ground-truth black-box objective for subsequent experimentation.

To systematically examine the effects of posterior tempering across different acquisition functions, we evaluate each method over real values of  $g \in \{0, 0.5, 1, 1.5, 2\}$ . <sup>1</sup> In

<sup>1</sup>Because non-integer values of  $g$  do not have easy to compute closed form solutions, we did not consider real-valued  $g$  case in the large-scale simulation study in Section 6.1.

Table 3: Bayesian optimization performance by Acquisition Function and  $\alpha$ . Entries are average best observed SQUID voltage across all 10 independent seeds at iterations 5-30.

Acquisition $g$	$\alpha$	iter5	iter10	iter15	iter20	iter25	iter30
MES	1	<b>5.24</b>	<b>5.54</b>	<b>5.69</b>	5.91	<b>6.29</b>	<b>6.54</b>
	Tempered	5.05	5.16	5.55	<b>6.02</b>	6.02	6.11
0.0	1	<b>5.07</b>	5.22	5.34	5.34	5.39	5.39
	Tempered	4.99	<b>5.51</b>	<b>5.99</b>	<b>5.99</b>	<b>6.26</b>	<b>6.26</b>
0.5	1	<b>5.44</b>	<b>6.09</b>	6.14	6.65	6.83	6.83
	Tempered	5.43	5.98	<b>7.00</b>	<b>7.02</b>	<b>7.02</b>	<b>7.05</b>
1.0	1	<b>5.29</b>	<b>5.44</b>	5.71	5.79	6.01	6.21
	Tempered	5.20	5.20	<b>5.85</b>	<b>6.86</b>	<b>7.19</b>	<b>7.26</b>
1.5	1	5.13	5.40	5.57	5.68	5.68	5.81
	Tempered	5.13	5.40	<b>5.94</b>	<b>6.05</b>	<b>6.05</b>	<b>6.05</b>
2.0	1	<b>5.75</b>	<b>6.40</b>	<b>6.40</b>	<b>6.69</b>	<b>7.28</b>	<b>7.44</b>
	Tempered	5.51	5.72	5.77	6.71	6.71	6.77

additional to the  $g$ -EI family, we also include the Max-value Entropy Search (MES) acquisition function, which can be viewed as a variational approximation to MES (Cheng et al., 2025). We consider the standard GP posterior ( $\alpha = 1$ ) and the tempered posterior described in Section 5. For each combination of  $\alpha$  and acquisition function, we conducted 10 independent random seeds of simulations, each with different initial sample size of 5.

Table 3 compares the average best-observed SQUID voltages under different acquisition functions and tempering level  $\alpha$ . Tempering yields only marginal gains for MES, suggesting that when the acquisition function is already highly exploratory, additional variance tempering provides limited benefit. In contrast, tempering substantially improve the performance for the  $g = 0$  case, consistent with our earlier findings in Section 6.1 that tempered posteriors enhance probability-improvement behavior by promoting benign exploration. Moderate gains are also observed for  $g \in \{0.5, 1, 1.5\}$ , indicating that tempering remains advantageous when the acquisition balances exploration and exploitation. Notably, for  $g = 2$ , tempering again provides no improvement, reinforcing the pattern that excessive exploration diminishes the utility of posterior tempering.

Figure 4 illustrates how the best-observed SQUID voltage evolves across iterations under varying acquisition functions and tempering levels. Each panel clearly shows the divergence between tempered and non-tempered trajectories, with the solid lines representing the progression of the median best observed voltage across all trials. The visual trend highlights that tempering generally accelerates the rise in best-observed values, particularly for moderate or low-exploration acquisitions, while can be potentially harmful for highly exploratory settings (e.g. , MES ,  $g = 2$ ).

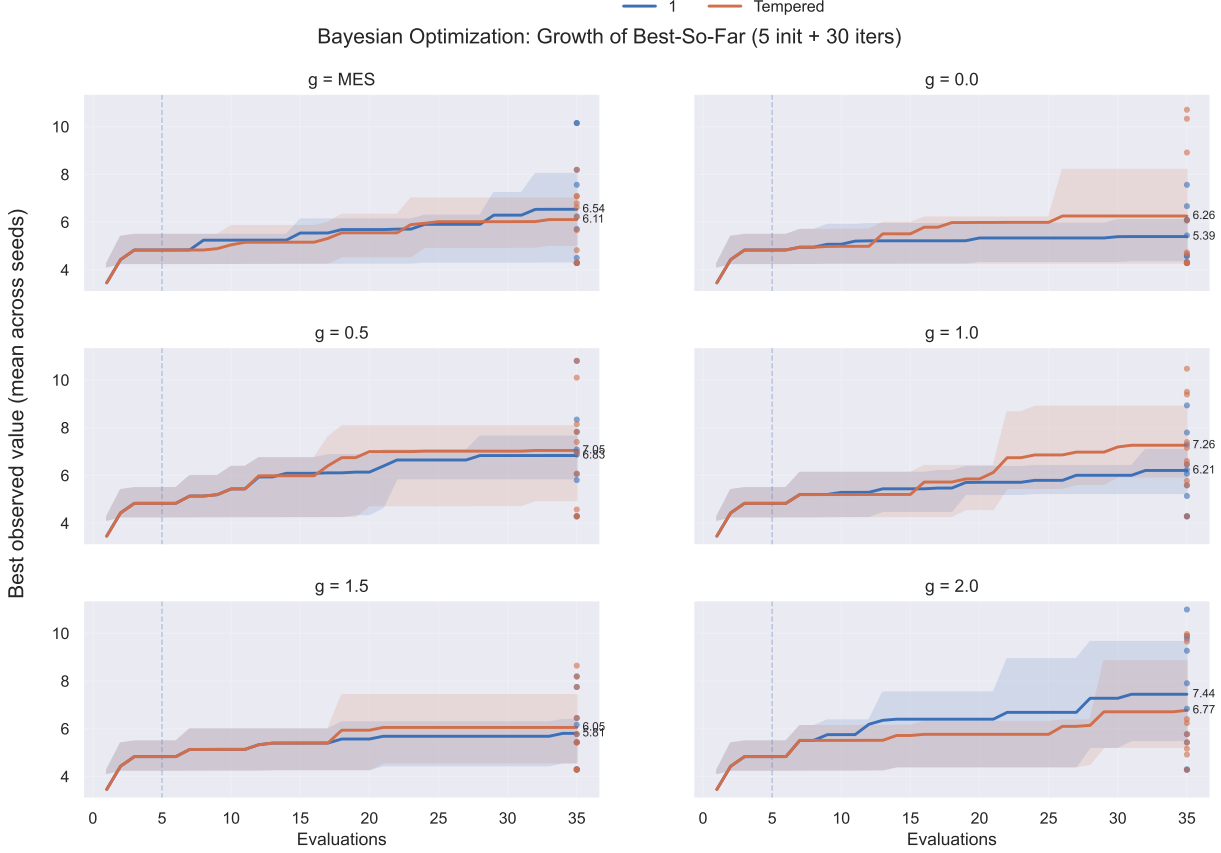


Figure 4: Effects of Tempering across Acquisition Functions: Iterations v.s. Best Observed SQUID Voltage

*Notes.* Ribbons are the 25-75% interquartile range across seeds at each iteration. The dots at the right edge represent the best observed voltage for a single BO trial, and the numbers annotate the terminal *median* best observed voltage across all trials.

## 7 Discussion

We study Bayesian optimization with tempered posterior surrogates and generalized expected improvement acquisition functions, where the likelihood power  $\alpha \in (0, 1]$  regulates how strongly each new evaluation updates the surrogate and the exponent  $g$  interpolates between probability of improvement and classic expected improvement. Our regret analysis for GP surrogates makes the dependence on  $(\alpha, g)$  explicit through information-gain quantities arising from improvement-based selection, thereby clarifying how tempering can be beneficial for BO. Building on this theory that connects acquisition-level and surrogate-level robustness, we further propose a sequential tuning-light schedule for choosing  $\alpha_t$ , which converges toward one as predictive calibration improves. Empirically, we show that tempering tends to stabilize improvement-based BO in regimes where the surrogate can become overconfident under localized sampling, with the largest gains typically observed for more exploitative policies (e.g., probability of improvement).

Our theoretical development focuses on generalized improvement-based acquisitions (the  $g$ -EI family) together with linear and GP surrogates. There are several potential extensions of our work. First, it would be of interest to understand whether likelihood tempering yields analogous benefits for other acquisition functions, such as knowledge gradient (Frazier et al., 2009) and entropy-based criteria (e.g., maximum-entropy search). Second, it remains open to derive regret guarantees for tempered updates when the surrogate departs from GP regression and scalar outputs, including tree-based (Boyne et al., 2025; Luo et al., 2024; O'Hagan et al., 2024), neural-network surrogates (Srinivas et al., 2009) and tensor-functional outputs (Luo et al., 2025). Third, while our analysis treats  $(\alpha, g)$  as fixed, developing methods that learn joint schedules  $(\alpha_t, g_t)$  based on the current design with finite-time guarantees would strengthen the connection between acquisition-level exploration and surrogate-level tempering trade-offs, even in BOI settings described in (Wang et al., 2025). More broadly, the perspective of tempering as an online learning-rate mechanism may extend beyond BO to other sequential decision problems, including reinforcement learning (Sutton and Barto, 2018), dynamic treatment regimes (Murphy, 2003), and adaptive experimental design and testing (Li et al., 2025; Rainforth et al., 2024; Srinivas et al., 2009). Finally, it would be valuable to understand how tempering interacts with recent advances targeting challenging BO regimes, such as in high-dimensional domains, nonsmooth or nonstationary objectives, and mixed discrete-continuous search spaces, where complementary tools and benchmarks are actively being developed (Cho et al., 2025; Luo et al., 2022, 2024; Noack et al., 2025; Risser et al., 2024).

## Disclosure statement

HL was supported by U.S. Department of Energy under Contract DE-AC02-05CH11231 and U.S. National Science Foundation NSF-DMS 2412403. Data and code have been made available at the following URL: <https://github.com/JiguangLi/Bayesian-Optimization-via-Tempered-Posterior>.

## References

Pierre Alquier and James Ridgway. Concentration of tempered posteriors and of their variational approximations. *The Annals of Statistics*, 48(3):1475–1497, 2020. doi: 10.1214/19-AOS1855.

Caroline Benjamins and Marius Lindauer. Self-adjusting weighted expected improvement for bayesian optimization. In *Proc. MLSys (PMLR Volume 224)*, 2023.

Anirban Bhattacharya, Debdeep Pati, and Yun Yang. Bayesian fractional posteriors. *The Annals of Statistics*, 47(1):39–66, 2019. doi: 10.1214/18-AOS1712.

Pier Giovanni Bissiri, Chris C Holmes, and Stephen G Walker. A general framework for updating belief distributions. *Journal of the Royal Statistical Society: Series B*, 78(5):1103–1130, 2016. doi: 10.1111/rssb.12158.

Toby Boyne, Jose Pablo Folch, Robert M Lee, Behrang Shafei, and Ruth Misener. Bark: A fully bayesian tree kernel for black-box optimization. *arXiv preprint arXiv:2503.05574*, 2025.

Eric Brochu, Matthew W. Hoffman, and Nando de Freitas. Portfolio allocation for bayesian optimization. In *UAI*, 2010.

Nuojin Cheng, Leonard Papenmeier, Stephen Becker, and Luigi Nardi. A unified framework for entropy search and expected improvement in bayesian optimization. *arXiv preprint arXiv:2501.18756*, 2025.

Younghyun Cho, James Demmel, Michał Dereziński, Haoyun Li, Hengrui Luo, Michael Mahoney, and Riley Murray. Surrogate-based autotuning for randomized sketching algorithms in regression problems. *SIAM Journal on Matrix Analysis and Applications*, 46(2):1247–1279, 2025.

Rianne de Heide, Alisa Kirichenko, Nishant A. Mehta, and Peter D. Grünwald. Safe-bayesian generalized linear regression. In *Proceedings of the 23rd International Conference on Artificial Intelligence and Statistics*, volume 108 of *Proceedings of Machine Learning Research*, pages 1791–1801. PMLR, 2020.

Peter Frazier, Warren Powell, and Savas Dayanik. The knowledge-gradient policy for correlated normal beliefs. *INFORMS journal on Computing*, 21(4):599–613, 2009.

Nial Friel and Antony N. Pettitt. Marginal likelihood estimation via power posteriors. *Journal of the Royal Statistical Society: Series B*, 70(3):589–607, 2008. doi: 10.1111/j.1467-9868.2007.00650.x.

Roman Garnett. *Bayesian Optimization*. Cambridge University Press, 2023.

Abhik Ghosh and Ayanendranath Basu. Robust bayes estimation using the density power divergence. *Annals of the Institute of Statistical Mathematics*, 68(2):413–437, 2016. doi: 10.1007/s10463-014-0499-0.

Daniel Golovin, Benjamin Solnik, Subhodeep Moitra, Greg Kochanski, John Karro, and David Sculley. Google vizier: A service for black-box optimization. In *Proceedings of the 23rd ACM SIGKDD international conference on knowledge discovery and data mining*, pages 1487–1495, 2017.

Robert B Gramacy. *Surrogates: Gaussian process modeling, design, and optimization for the applied sciences*. Chapman and Hall/CRC, 2020.

Peter Grünwald. The safe bayesian: learning the learning rate via the mixability gap. In *Algorithmic Learning Theory*, volume 7568 of *Lecture Notes in Computer Science*, pages 169–183. Springer, 2012. doi: 10.1007/978-3-642-34106-9\_16.

Peter D. Grünwald and Thijs Van Ommen. Inconsistency of bayesian inference for misspecified linear models, and a proposal for repairing it. *Bayesian Analysis*, 12(4):1069–1103, 2017. doi: 10.1214/17-BA1091.

Chris C Holmes and Stephen G Walker. Assigning a value to a power likelihood in a general bayesian model. *Biometrika*, 104(2):497–503, 2017.

Daniel Hsu, Sham Kakade, and Tong Zhang. A tail inequality for quadratic forms of subgaussian random vectors. *Electronic Communications in Probability*, 17:1–6, 2012. doi: 10.1214/ECP.v17-2079.

Shouri Hu, Haowei Wang, Zhongxiang Dai, Bryan Kian Hsiang Low, and Szu Hui Ng. Adjusted expected improvement for cumulative regret minimization in noisy bayesian optimization. *Journal of Machine Learning Research*, 26(46):1–33, 2025.

D. Huang, T. T. Allen, W. I. Notz, and R. A. Miller. Sequential kriging optimization using multiple-fidelity evaluations. *Structural and Multidisciplinary Optimization*, 32(5):369–382, 2006.

Prateek Jaiswal, Debdeep Pati, Anirban Bhattacharya, and Bani K Mallick. Generalized regret analysis of thompson sampling using fractional posteriors. *arXiv preprint arXiv:2309.06349*, 2023.

B. J. K. Kleijn and A. W. van der Vaart. The bernstein–von mises theorem under misspecification. *Electronic Journal of Statistics*, 6:354–381, 2012. doi: 10.1214/12-EJS675.

Jeremias Knoblauch, James Jewson, and Theodoros Damoulas. An optimization-centric view on bayes’ rule: Variational bayes and beyond. *Journal of Machine Learning Research*, 23(132):1–109, 2022.

A. G. Kusne, H. Yu, C. Wu, H. Zhang, J. Hattrick-Simpers, B. DeCost, S. Sarker, C. Oses, S. Curtarolo, I. Takeuchi, et al. On-the-fly closed-loop materials discovery via Bayesian active learning. *Nature Communications*, 11(1):5966, 2020. doi: 10.1038/s41467-020-19597-w. URL <https://doi.org/10.1038/s41467-020-19597-w>.

Benjamin Letham, Brian Karrer, Guilherme Ottoni, and Eytan Bakshy. Constrained bayesian optimization with noisy experiments. *Bayesian Analysis*, 14(2):495–519, 2019.

Jiguang Li, Robert Gibbons, and Veronika Rockova. Deep computerized adaptive testing, 2025. URL <https://arxiv.org/abs/2502.19275>.

C. J. Long, J. Hattrick-Simpers, M. Murakami, R. C. Srivastava, I. Takeuchi, V. L. Karen, and X. Li. Rapid structural mapping of ternary metallic alloy systems using the combinatorial approach and cluster analysis. *Review of Scientific Instruments*, 78(7):072217, July 2007. doi: 10.1063/1.2755487. URL <https://doi.org/10.1063/1.2755487>.

Hengrui Luo, Giovanni Nattino, and Matthew T Pratola. Sparse additive gaussian process regression. *Journal of Machine Learning Research*, 23(61):1–34, 2022.

Hengrui Luo, Younghyun Cho, James W Demmel, Xiaoye S Li, and Yang Liu. Hybrid parameter search and dynamic model selection for mixed-variable bayesian optimization. *Journal of Computational and Graphical Statistics*, 33(3):855–868, 2024.

Hengrui Luo, Akira Horiguchi, and Li Ma. Efficient decision trees for tensor regressions. *Journal of Computational and Graphical Statistics*, (just-accepted):1–39, 2025.

Simon P Lyddon, Chris C Holmes, and Stephen G Walker. General bayesian updating and the loss-likelihood bootstrap. *Biometrika*, 106(2):465–478, 2019. doi: 10.1093/biomet/azs006.

Jeffrey W. Miller and David B. Dunson. Robust bayesian inference via coarsening. *Journal of the American Statistical Association*, 114(527):1113–1125, 2019. doi: 10.1080/01621459.2018.1469995.

Jonas Močkus. On bayesian methods for seeking the extremum. In *IFIP Technical Conference on Optimization Techniques*, pages 400–404. Springer, 1974.

S. A. Murphy. Optimal dynamic treatment regimes. *Journal of the Royal Statistical Society Series B: Statistical Methodology*, 65(2):331–355, 04 2003. ISSN 1369-7412. doi: 10.1111/1467-9868.00389. URL <https://doi.org/10.1111/1467-9868.00389>.

Marcus M Noack, Mark D Risser, Hengrui Luo, Vardaan Tekriwal, and Ronald J Pandolfi. gp2scale: A class of compactly-supported non-stationary kernels and distributed computing for exact gaussian processes on 10 million data points. *arXiv preprint arXiv:2512.06143*, 2025.

Sean O’Hagan, Jungeum Kim, and Veronika Rockova. Tree bandits for generative bayes, 2024. URL <https://arxiv.org/abs/2404.10436>.

Konstantinos Pitas and Julyan Arbel. The fine print on tempered posteriors. In *Asian Conference on Machine Learning*, pages 1087–1102. PMLR, 2024.

Chongli Qin, Daniel Russo, and Benjamin Van Roy. Improving the expected improvement algorithm. In *NeurIPS*, 2017.

Tom Rainforth, Adam Foster, Desi R. Ivanova, and Freddie Bickford Smith. Modern Bayesian Experimental Design. *Statistical Science*, 39(1):100 – 114, 2024. doi: 10.1214/23-STS915. URL <https://doi.org/10.1214/23-STS915>.

Mark D Risser, Marcus M Noack, Hengrui Luo, and Ronald Pandolfi. Compactly-supported nonstationary kernels for computing exact gaussian processes on big data. *arXiv preprint arXiv:2411.05869*, 2024.

Matthias Schonlau, William J Welch, and Donald R Jones. Global versus local search in constrained optimization of computer models. *Lecture notes-monograph series*, pages 11–25, 1998.

Bobak Shahriari, Ziyu Wang, Matthew W. Hoffman, Alexandre Bouchard-Côté, and Nando de Freitas. An entropy search portfolio for bayesian optimization. *arXiv:1406.4625*, 2014.

Niranjan Srinivas, Andreas Krause, Sham M Kakade, and Matthias Seeger. Gaussian process optimization in the bandit setting: No regret and experimental design. *arXiv preprint arXiv:0912.3995*, 2009.

Niranjan Srinivas, Andreas Krause, Sham M Kakade, and Matthias W Seeger. Information-theoretic regret bounds for gaussian process optimization in the bandit setting. *IEEE transactions on information theory*, 58(5):3250–3265, 2012.

S. Surjanovic and D. Bingham. Virtual library of simulation experiments: Test functions and datasets. Retrieved October 25, 2025, from <http://www.sfu.ca/~ssurjano>.

Richard S. Sutton and Andrew G. Barto. *Reinforcement Learning: An Introduction*. The MIT Press, second edition, 2018. URL <http://incompleteideas.net/book/the-book-2nd.html>.

Nicholas Syring and Ryan Martin. Calibrating generalized posterior credible regions. *Biometrika*, 106(2):479–486, 2019. doi: 10.1093/biomet/asz007.

Jingyi Wang, Haowei Wang, Szu Hui Ng, and Cosmin G Petra. Bayesian optimization with expected improvement: No regret and the choice of incumbent. *arXiv preprint arXiv:2508.15674*, 2025.

Ziyu Wang and Nando de Freitas. Theoretical analysis of bayesian optimisation with unknown gaussian process hyper-parameters, 2014. URL <https://arxiv.org/abs/1406.7758>.

Sumio Watanabe. A widely applicable bayesian information criterion. *Journal of Machine Learning Research*, 14:867–897, 2013.

Pei-Shien Wu and Ryan Martin. A comparison of learning rate selection methods in generalized bayesian inference. *Bayesian Analysis*, 18(1):105–132, 2023.

Yun Yang, Debdeep Pati, and Anirban Bhattacharya.  $\alpha$ -variational inference with statistical guarantees. *The Annals of Statistics*, 48(2):886–905, 2020. doi: 10.1214/19-AOS1827.

# SUPPLEMENTARY MATERIALS

## A Additional Motivation Results

$\alpha$	df = 1	df = 2	df = 5	df = 10	df = 20	df = 100
0.1	<b>0.9963</b>	<b>0.9875</b>	<b>0.9856</b>	<b>0.9857</b>	<b>0.9857</b>	<b>0.9857</b>
0.5	0.9848	0.7644	0.7687	0.7608	0.7631	0.7631
1.0	0.9665	0.7737	0.9842	0.9846	0.9848	0.9850

Table 4: Best observed  $y$  from PI runs for each  $(\alpha, \text{df})$ . Maximum per column is bold.

$\alpha$	df = 1	df = 2	df = 5	df = 10	df = 20	df = 100
0.1	0.9787	0.9844	0.9919	0.9909	0.9904	0.9899
0.5	<b>1.3515</b>	<b>0.9901</b>	<b>1.0000</b>	<b>0.9957</b>	<b>0.9940</b>	<b>0.9925</b>
1.0	0.9875	0.9852	0.9883	0.9879	0.9879	0.9878

Table 5: Best observed  $y$  from EI runs for each  $(\alpha, \text{df})$ . Maximum per column is bold.

Figure 2 in the main text presents a controlled one dimensional example in which three values of the tempering parameter  $\alpha \in \{0.1, 0.5, 1.0\}$  are used with probability of improvement. The figure shows that when the surrogate is fit with a tempered posterior with small  $\alpha$ , the posterior variance is effectively enlarged and the probability of improvement curve places mass in regions that have not yet been explored. As a result the policy that uses  $\alpha = 0.1$  is able to locate a point with noticeably larger observed value than the policies that keep  $\alpha = 0.5$  or  $\alpha = 1.0$ . We interpret this as evidence that tempering can counter posterior over confidence and can restore exploratory moves when the acquisition is otherwise very exploitative.

In BO, model misspecification and the reuse of surrogate fits across iterations can make the GP posterior too sharp. A natural question is therefore whether the effect persists once we move away from the convenient Gaussian noise. The additional experiment keeps (3), the same acquisition, but it replaces the Gaussian noise by Student  $t$  noise with several degrees of freedom  $\alpha$ .

Table 4 reports the best value of the observed response that each of the three tempered policies attains, across degrees of freedom equal to 1, 2, 5, 10, 20, 100. For every column the largest value is obtained by  $\alpha = 0.1$ . The advantage is most pronounced for degrees of freedom equal to 1 and 2, which correspond to the heaviest tails and therefore to the strongest mismatch. For larger degrees of freedom, the values for  $\alpha = 0.1$  and  $\alpha = 1.0$  become close, which is expected because the Student  $t$  noise approaches a Gaussian distribution and the original example already showed that the untempered policy can perform reasonably in that case.

Table 5 reports the analogous experiment for expected improvement. In that case the maximum in each column is obtained for  $\alpha = 0.5$ . This agrees with the broader empirical conclusions of the paper, where it is noted that acquisitions that are already more balanced between exploitation and exploration benefit from a moderate amount of tempering but do not require the very small values of  $\alpha$  that were effective for probability of improvement.

This set of additional experiment shows that the main effect described in the text is acquisition dependent. For the strongly exploitative rule the smallest  $\alpha$  is best, and for the more balanced rule an intermediate  $\alpha$  is preferable. This is in harmony with the interpretation in the main text that tempered posteriors act as a control on the effective confidence of the surrogate.

## B Connection to Stochastic Gradient Descent

This subsection presents an exact per iteration equality that links the  $\alpha$  tempered Gaussian process update of the posterior mean with a single preconditioned stochastic gradient step on a one point loss. The statement holds for Gaussian observation noise and is conditional on the kernel fitted at the previous iteration, which is the convention adopted in sequential GP regression.

Consider an unknown target  $f^*$  and noisy observations  $y_t = f^*(x_t) + \varepsilon_t$  with  $\varepsilon_t \sim \mathcal{N}(0, \sigma^2)$ . Let the prior be  $f \sim \mathcal{GP}(0, k)$  and after  $t-1$  steps write the posterior as  $\mathcal{GP}(\mu_{t-1}, k_{t-1})$ . For a candidate input location  $x$  denote the predictive variance by  $v_{t-1}(x) := k_{t-1}(x, x)$  and the cross covariance by  $c_{t-1}(x, x_t) := k_{t-1}(x, x_t)$ . At step  $t$  temper the likelihood by a factor  $\alpha_t > 0$ . Since the likelihood is Gaussian, tempering is equivalent to replacing the noise variance by  $\sigma^2/\alpha_t$ . The standard conditioning formula then yields the one point update of the mean

$$\mu_t(x) = \mu_{t-1}(x) + \frac{c_{t-1}(x, x_t)}{v_{t-1}(x_t) + \sigma^2/\alpha_t} (y_t - \mu_{t-1}(x_t)). \quad (11)$$

It is convenient to factor the gain as a scalar times a direction,

$$\frac{c_{t-1}(x, x_t)}{v_{t-1}(x_t) + \sigma^2/\alpha_t} = \eta_t(\alpha_t) c_{t-1}(x, x_t), \quad \eta_t(\alpha_t) = \frac{\alpha_t}{\sigma^2 + \alpha_t v_{t-1}(x_t)}. \quad (12)$$

Substituting (12) into (11) gives the compact form

$$\mu_t = \mu_{t-1} + \eta_t(\alpha_t) (y_t - \mu_{t-1}(x_t)) c_{t-1}(\cdot, x_t). \quad (13)$$

Now consider a functional optimization view at step  $t$  based on the one point objective

$$\mathcal{J}_t(g) = \frac{\alpha_t}{2\sigma^2} (y_t - g(x_t))^2 + \frac{1}{2} \|g - \mu_{t-1}\|_{\mathcal{H}_{k_{t-1}}}^2, \quad (14)$$

where  $\mathcal{H}_{k_{t-1}}$  is the reproducing kernel Hilbert space associated with  $k_{t-1}$ . The negative log of the tempered posterior is equal to  $\mathcal{J}_t$  up to an additive constant, so the minimizer of (14) coincides with the tempered posterior mean. By the representer theorem the minimizer has the form  $g = \mu_{t-1} + \beta c_{t-1}(\cdot, x_t)$ . Differentiation with respect to  $\beta$  and evaluation at zero derivative give

$$\beta^* = \frac{\alpha_t}{\sigma^2 + \alpha_t v_{t-1}(x_t)} (y_t - \mu_{t-1}(x_t)) = \eta_t(\alpha_t) (y_t - \mu_{t-1}(x_t)). \quad (15)$$

Substituting  $g = \mu_{t-1} + \beta^* c_{t-1}(\cdot, x_t)$  leads exactly to the update in (13). Hence the tempered

Gaussian update with  $g$ -EI equals a single preconditioned stochastic gradient step with direction  $c_{t-1}(\cdot, x_t)$  and learning rate  $\eta_t(\alpha_t)$  applied to the loss (14).

We summarize the per iteration correspondence for a fixed datum  $(x_t, y_t)$  for the mean function  $\mu_t$ :

$$\text{tempered update with parameter } \alpha_t \iff (16)$$

$$\text{stochastic gradient step with learning rate } \eta_t(\alpha_t) = \frac{\alpha_t}{\sigma^2 + \alpha_t v_{t-1}(x_t)}. \quad (17)$$

When  $\alpha_t$  is small the step is conservative and the mean update is close to the previous iterate, while large  $\alpha_t$  values produce aggressive updates that are limited by the local variance  $v_{t-1}(x_t)$ .

This identity is an equality of model updates that applies once the location  $x_t$  and the observation  $y_t$  are given, and shares a very similar form of robust tempering (Holmes and Walker, 2017). If a stochastic gradient method is supplied with the same sequence of data pairs then (13) ensures that the two procedures produce the same mean path at the granularity of single iterations.

## C Linear Surrogate BO Algorithm

---

**Algorithm 1** TEMPERED-EI BAYESIAN OPTIMIZATION (LINEAR SURROGATE)

---

**Require:** Compact domain  $\mathcal{X} \subset \mathbb{R}^p$ ; feature map  $\psi : \mathcal{X} \rightarrow \mathbb{R}^d$  with  $\|\psi(x)\|_2 \leq L$ ; prior precision  $\lambda > 0$ ; noise std.  $\sigma > 0$ ;

budget  $T \in \mathbb{N}$ ; initial design  $\{(x_s, y_s)\}_{s=1}^{t_0}$  (possibly  $t_0 = 0$ ); tempering policy  $\alpha_t \in (0, 1]$

**Ensure:** Sequence  $\{x_t\}_{t=1}^T$  and incumbent  $\hat{x}^* \in \arg \max_{x \in \mathcal{X}} \mu_{T, \alpha_T}(x)$

1:  $t \leftarrow t_0$ ;  $\mathcal{D}_t \leftarrow \{(x_s, y_s)\}_{s=1}^t$ ;  $X_t \leftarrow [\psi(x_1), \dots, \psi(x_t)]^\top$ ;  $y_{1:t} \leftarrow (y_1, \dots, y_t)^\top$

2: **while**  $t < T$  **do**

3: Pick tempering  $\alpha_{t+1} \in (0, 1]$  via a policy (e.g. fixed  $\alpha$ , or TEMPERSCHEDEULE)

4: **Posterior update** w.r.t.  $\alpha_{t+1}$  (Alg. 3): compute

$$V_{t+1, \alpha} = \lambda I_d + \frac{\alpha_{t+1}}{\sigma^2} X_t^T X_t, \quad \Sigma_{t+1, \alpha} = V_{t+1, \alpha}^{-1}, \quad \mu_{t+1, \alpha} = \Sigma_{t+1, \alpha} \frac{\alpha_{t+1}}{\sigma^2} X_t^T y_{1:t}.$$

5: Define predictive mean/variance for any  $x \in \mathcal{X}$ :

$$\mu_{t+1, \alpha}(x) = \psi(x)^\top \mu_{t+1, \alpha}, \quad \sigma_{t, \alpha_{t+1}}^2(x) = \psi(x)^\top \Sigma_{t+1, \alpha} \psi(x).$$

6: Compute current mean-maximum  $m_t := \max_{x \in \mathcal{X}} \mu_{t, \alpha_{t+1}}(x)$  (*global or over a candidate set*)

7: **Acquisition:** define  $\text{EI}_{t, \alpha_{t+1}}(x)$  via Alg. 4  $g = 1$ ; pick

$$x_{t+1} \in \arg \max_{x \in \mathcal{X}} \text{EI}_{t, \alpha_{t+1}}(x).$$

8: Query black-box:  $y_{t+1} \leftarrow f(x_{t+1}) + \epsilon_{t+1}$  with  $\epsilon_{t+1} \sim \mathcal{N}(0, \sigma^2)$

9: Augment data:  $\mathcal{D}_{t+1} \leftarrow \mathcal{D}_t \cup \{(x_{t+1}, y_{t+1})\}$ ;  $X_{t+1} \leftarrow \begin{bmatrix} X_t \\ \psi(x_{t+1})^\top \end{bmatrix}$ ;  $y_{1:t+1} \leftarrow (y_{1:t}, y_{t+1})$

10:  $t \leftarrow t + 1$

11: **end while**

12: **return**  $\hat{x}^* \in \arg \max_{x \in \mathcal{X}} \mu_{T, \alpha_T}(x)$  (*or the best observed  $y_t$ -incumbent*)

---

## D Proof of Linear Regret Bounds

### D.1 Proof of Lemma 3.2

*Proof.* By Sylvester's theorem,  $\frac{\det V_{T, \alpha}}{\det(\lambda I_d)} = \det(I_d + \frac{\alpha}{\lambda \sigma^2} X_T^T X_T) = \prod_{j=1}^d (1 + \eta_j)$ , where  $\eta_j \geq 0$  are eigenvalues of  $\frac{\alpha}{\lambda \sigma^2} X_T^T X_T$  and  $\sum_j \eta_j = \frac{\alpha}{\lambda \sigma^2} \text{tr}(X_T^T X_T) \leq \frac{\alpha L^2 T}{\lambda \sigma^2}$ . Concavity of  $\log(1 + x)$  and Jensen give the bound.  $\square$

### D.2 UCB Argument

Due to Assumption 1, it suffices to study the regret bound of upper confidence bound acquisition by Lemma D.2. Define the filtration  $\mathcal{F}_t := \sigma(x_1, \epsilon_1, \dots, x_t, \epsilon_t)$ , the standardized

noise

$$\xi_t := \epsilon_t / \sigma \sim \mathcal{N}(0, 1) \text{ i.i.d.},$$

and the rescaled features  $z_t := \frac{\sqrt{\alpha}}{\sigma} \psi(x_t) \in \mathbb{R}^d$ . Let  $Z_t = [z_1, \dots, z_t]^\top$  and

$$W_t := \sum_{i=1}^t z_i \xi_i = Z_t^T \xi_{1:t} \in \mathbb{R}^d, \quad V_{T,\alpha} = \lambda I_d + Z_t^T Z_t.$$

We begin by introducing two auxilliary lemmas:

**Lemma D.1** (Coordinate-wise monotonicity of EI). *Let  $\text{EI}(\mu, \sigma; m) = (\mu - m)\Phi\left(\frac{\mu-m}{\sigma}\right) + \sigma\phi\left(\frac{\mu-m}{\sigma}\right)$ . For all  $\mu \in \mathbb{R}$ ,  $\sigma > 0$ ,*

$$\frac{\partial}{\partial \mu} \text{EI}(\mu, \sigma; m) = \Phi\left(\frac{\mu-m}{\sigma}\right) \geq 0, \quad \frac{\partial}{\partial \sigma} \text{EI}(\mu, \sigma; m) = \phi\left(\frac{\mu-m}{\sigma}\right) \geq 0.$$

*Proof.* Differentiate the closed form using  $\frac{\partial}{\partial \mu}(\mu - m) = 1$ ,  $\frac{\partial}{\partial \mu}\left(\frac{\mu-m}{\sigma}\right) = \frac{1}{\sigma}$ ,  $\frac{\partial}{\partial \sigma}\left(\frac{\mu-m}{\sigma}\right) = -\frac{\mu-m}{\sigma^2}$ ,  $\Phi' = \phi$  and  $\phi' = -z\phi$ .  $\square$

For example, if the set  $\{(\mu_{t-1,\alpha}(x), \sigma_{t-1,\alpha}(x)) : x \in \mathcal{X}\}$  inside  $\{\mu \leq m_{t-1}\}$  lies on a nonincreasing curve  $h(\cdot)$  such that  $\sigma = h(\mu)$ , then by Lemma D.1 the order induced by any increasing function of  $(\mu, \sigma)$  (such as EI or  $\mu + \kappa\sigma$  with  $\kappa \geq 0$ ) is the same along that curve.

**Lemma D.2** (Argmax equivalence under alignment). *If Assumption 2 holds, then every EI maximizer is also a maximizer of the linear score*

$$\text{sc}_{t-1,\kappa_t}(x) := \mu_{t-1,\alpha}(x) + \kappa_t \sigma_{t-1,\alpha}(x).$$

*Proof.* Let  $x_t \in \arg \max \text{EI}_{t-1,\alpha}$ . If some  $x$  satisfies  $\text{sc}_{t-1,\kappa_t}(x) > \text{sc}_{t-1,\kappa_t}(x_t)$  with both means  $\leq m_{t-1}$ , Assumption 2 implies  $\text{EI}_{t-1,\alpha}(x) > \text{EI}_{t-1,\alpha}(x_t)$ , a contradiction.  $\square$

**Lemma D.3** (Self-normalized bound). *For  $\delta \in (0, 1)$ , with probability  $\geq 1 - \delta$ , simultaneously for all  $t \geq 0$ ,*

$$\|W_t\|_{V_{t,\alpha}^{-1}}^2 \leq 2 \log\left(\frac{\det(V_{t,\alpha})^{1/2}}{\det(\lambda I_d)^{1/2} \delta}\right).$$

*Proof.* Consider  $L_t(\theta) := \exp(\theta^T W_t - \frac{1}{2}\|\theta\|_{V_{t,\alpha}}^2)$ . As in standard proofs,  $\{L_t(\theta)\}$  is a martingale for each fixed  $\theta \in \mathbb{R}^d$  because conditionally on  $\mathcal{F}_{t-1}$ ,  $W_t = W_{t-1} + z_t \xi_t$  and  $\mathbb{E}[e^{(\theta^T z_t)\xi_t - \frac{1}{2}(\theta^T z_t)^2}] = 1$  for  $\xi_t \sim \mathcal{N}(0, 1)$ . Mix with  $\Theta \sim \mathcal{N}(0, \lambda^{-1} I_d)$  (independent) to obtain a nonnegative martingale

$$M_t := \frac{\det(\lambda I_d)^{1/2}}{\det(V_{t,\alpha})^{1/2}} \exp\left(\frac{1}{2}\|W_t\|_{V_{t,\alpha}^{-1}}^2\right),$$

with  $\mathbb{E}M_t = 1$ . Ville's inequality gives

$$\mathbb{P}\left(\exists t : \frac{1}{2}\|W_t\|_{V_{t,\alpha}^{-1}}^2 \geq \log \frac{\det(V_{t,\alpha})^{1/2}}{\det(\lambda I_d)^{1/2} \delta}\right) \leq \delta,$$

which is the claim.  $\square$

**Lemma D.4** (Uniform linear  $\alpha$ -confidence). *With probability  $\geq 1 - \delta$ , for all  $t \geq 0$  and  $x \in \mathcal{X}$ ,*

$$|f(x) - \mu_{t,\alpha}(x)| \leq \beta_t(\alpha, \delta) \sigma_{t,\alpha}(x), \quad \beta_t(\alpha, \delta) := \sqrt{\lambda} S_\theta + \sqrt{\alpha} \sqrt{\log \frac{\det V_{t,\alpha}}{\det(\lambda I_d)} + 2 \log \frac{1}{\delta}}.$$

*Proof.* From  $\mu_{t,\alpha} - \theta^* = \Sigma_{t,\alpha} \frac{\alpha}{\sigma^2} X_t^\top \epsilon_{1:t} - \lambda \Sigma_{t,\alpha} \theta^*$ ,

$$f(x) - \mu_{t,\alpha}(x) = \underbrace{\psi(x)^\top \lambda \Sigma_{t,\alpha} \theta^*}_A - \underbrace{\psi(x)^\top \Sigma_{t,\alpha} \frac{\alpha}{\sigma^2} X_t^\top \epsilon_{1:t}}_B.$$

We first apply Cauchy-Schwarz to  $A$  in the  $\|\cdot\|_{\Sigma_{t,\alpha}}$  norm. Since  $\theta^T \Sigma_{t,\alpha} \theta \leq \theta^T (\lambda^{-1} \mathbb{I}_d) \theta$ , this yields

$$A \leq \|\psi(x)\|_{\Sigma_{t,\alpha}} \|\lambda \theta^*\|_{\Sigma_{t,\alpha}} \leq \sigma_{t,\alpha}(x) \sqrt{\lambda} \|\theta^*\|_2 \leq \sigma_{t,\alpha}(x) \sqrt{\lambda} S_\theta.$$

We again apply Cauchy-Schwarz to  $B$  in the  $\|\cdot\|_{\Sigma_{t,\alpha}}$  norm. This yields

$$B \leq \|\psi(x)\|_{\Sigma_{t,\alpha}} \|\sqrt{\alpha} W_t\|_{\Sigma_{t,\alpha}} \leq \sigma_{t,\alpha}(x) \sqrt{\alpha} \|W_t\|_{V_{t,\alpha}^{-1}}.$$

Apply Lemma D.3 onto part B and multiply by  $\sigma/\sqrt{\alpha}$  will yield this bound.  $\square$

### D.3 Proof of the Theorem 3.1

**Lemma D.5.** *Let  $u_t := \psi(x_t)^\top V_{t-1,\alpha}^{-1} \psi(x_t)$ . Then*

$$\frac{\det V_{t,\alpha}}{\det V_{t-1,\alpha}} = 1 + \frac{\alpha}{\sigma^2} u_t, \quad \log \frac{\det V_{T,\alpha}}{\det(\lambda I_d)} = \sum_{t=1}^T \log \left( 1 + \frac{\alpha}{\sigma^2} u_t \right).$$

*Proof.* This is the matrix determinant lemma:  $\det(A + ab^\top) = \det(A) (1 + b^\top A^{-1} a)$ , applied to  $A = V_{t-1,\alpha}$  and  $a = b = \sqrt{\alpha} \psi(x_t)/\sigma$ .  $\square$

**Lemma D.6** (Accumulated posterior variance). *Let  $u_t := \psi(x_t)^\top V_{t-1,\alpha}^{-1} \psi(x_t)$ , then With  $z_t := \frac{\alpha}{\sigma^2} u_t \geq 0$ ,*

$$\sum_{t=1}^T u_t \leq \left( \frac{2\sigma^2}{\alpha} + \frac{L^2/\lambda}{\log 2} \right) \log \frac{\det V_{T,\alpha}}{\det(\lambda I_d)}.$$

*Proof.* Split indices into  $\mathcal{S} = \{t : z_t \leq 1\}$  and  $\mathcal{L} = \{t : z_t > 1\}$ . If  $z_t \leq 1$ , then  $z_t \leq 2 \log(1 + z_t)$ , hence  $u_t = \frac{\sigma^2}{\alpha} z_t \leq \frac{2\sigma^2}{\alpha} \log(1 + z_t)$ . If  $z_t > 1$ , then  $\log(1 + z_t) \geq \log 2$  and  $u_t \leq \psi(x_t)^\top (\lambda I_d)^{-1} \psi(x_t) \leq L^2/\lambda$ , so  $\sum_{t \in \mathcal{L}} u_t \leq \frac{L^2/\lambda}{\log 2} \sum_{t \in \mathcal{L}} \log(1 + z_t)$ . Sum both parts and use Lemma D.5 to yield the result.  $\square$

*Proof.* Working on the  $1 - \delta$  event of  $|f(x) - \mu_{t,\alpha}(x)| \leq \beta_t(\alpha, \delta) \sigma_{t,\alpha}(x)$ , (See Lemma D.4), for each  $t$  and all  $x$ ,

$$f(x) \leq \mu_{t-1,\alpha}(x) + \kappa_t \sigma_{t-1,\alpha}(x), \quad f(x) \geq \mu_{t-1,\alpha}(x) - \kappa_t \sigma_{t-1,\alpha}(x).$$

Thus

$$r_t = f(x^*) - f(x_t) \leq [\mu_{t-1,\alpha}(x^*) + \kappa_t \sigma_{t-1,\alpha}(x^*)] - [\mu_{t-1,\alpha}(x_t) - \kappa_t \sigma_{t-1,\alpha}(x_t)].$$

By Lemma D.2, the EI maximizer  $x_t$  maximizes  $sc_{t-1,\kappa_t}$ , hence  $\mu_{t-1,\alpha}(x^*) + \kappa_t \sigma_{t-1,\alpha}(x^*) \leq \mu_{t-1,\alpha}(x_t) + \kappa_t \sigma_{t-1,\alpha}(x_t)$ , and therefore  $r_t \leq 2\kappa_t \sigma_{t-1,\alpha}(x_t) \leq 2\beta_T(\alpha, \delta) \sigma_{t-1,\alpha}(x_t)$  since  $\beta_{t-1} \leq \beta_T$ . Sum over  $t$ , use Cauchy-Schwarz and Lemma D.6 to yield the result.  $\square$

## E GP Surrogate BO Algorithm

Special cases:  $g=0$  gives probability of improvement  $\Phi(-v)$ ;  $g=1$  recovers classical EI:  $gEI^{(1)} = \sigma(\phi(v) - v \Phi(-v))$ .

---

**Algorithm 2** BO- $\alpha$ GP-GEI: Bayesian Optimization via  $\alpha$ -Tempered GP Posterior and Generalized EI

---

**Require:** Domain  $\mathcal{X} \subset \mathbb{R}^p$ ; GP prior  $(m, k_\theta)$ ; noise variance  $\sigma^2 > 0$  (or estimator); budget  $T$ .

**Require:** Generalized-EI order  $g \in \{0, 1, 2, \dots\}$  (fixed), or a scheduler `GSCHEDULE` returning  $g_t$ .

**Require:** Tempering scheduler `TEMPERSCHEDULE` returning  $\alpha_t \in (0, 1]$  (e.g., fixed  $\alpha_t \equiv 1$ , or data-driven).

**Require:** (Optional) hyperparameter learning routine `FITHYPERPARAMS` (e.g., marginal likelihood).

- 1: Initialize design  $\{x_1, \dots, x_{t_0}\} \subset \mathcal{X}$  (space-filling or random); evaluate  $y_s = f(x_s) + \epsilon_s$ ,  $s = 1, \dots, t_0$ .
- 2: Set  $t \leftarrow t_0$ ;  $\mathcal{D}_t \leftarrow \{(x_s, y_s)\}_{s=1}^t$ .
- 3: **for**  $t = t_0, t_0+1, \dots, T-1$  **do**
- 4:    $\alpha_t \leftarrow \text{TEMPERSCHEDULE}(\mathcal{D}_t)$   $\triangleright \alpha_t \in (0, 1]$ ; e.g.,  $\alpha_t \equiv 1$
- 5:    $(\theta, m) \leftarrow \text{FITHYPERPARAMS}(\mathcal{D}_t)$   $\triangleright$  Optional re-fit kernel/mean
- 6:    $(\mu_{t,\alpha_t}, \sigma_{t,\alpha_t}) \leftarrow \text{TEMPEREDPOSTERIORGP}(\mathcal{D}_t, m, k_\theta, \sigma^2, \alpha_t)$
- 7:    $\mu_{t,\alpha_t}^+ \leftarrow \max_{x \in \mathcal{X}} \mu_{t,\alpha_t}(x)$   $\triangleright$  Global maximization or dense grid
- 8:    $g_t \leftarrow \text{GSCHEDULE}(t, \mathcal{D}_t)$  **or**  $g_t \leftarrow g$   $\triangleright$  Fixed or adaptive  $g$
- 9:   Define acquisition

$$a_t(x) \leftarrow \text{GEI}(\mu_{t,\alpha_t}(x), \sigma_{t,\alpha_t}(x), \mu_{t,\alpha_t}^+, g_t)$$

- 10:    $x_{t+1} \leftarrow \arg \max_{x \in \mathcal{X}} a_t(x)$   $\triangleright$  Global maximization of g-EI
- 11:   Query black-box:  $y_{t+1} \leftarrow f(x_{t+1}) + \epsilon_{t+1}$ , with  $\epsilon_{t+1} \sim \mathcal{N}(0, \sigma^2)$
- 12:   Augment data:  $\mathcal{D}_{t+1} \leftarrow \mathcal{D}_t \cup \{(x_{t+1}, y_{t+1})\}$
- 13: **end for**
- 14: **return**  $x_{\text{rec}} \in \arg \max_{s \in \{1, \dots, T\}} \mu_{T,\alpha_T}(x_s)$   $\triangleright$  Or best observed  $y_s$

---

---

**Algorithm 3** TEMPEREDPOSTERIORGP( $\mathcal{D}_t, m, k_\theta, \sigma^2, \alpha$ )

---

**Require:**  $\mathcal{D}_t = \{(x_s, y_s)\}_{s=1}^t$ , mean  $m$ , kernel  $k_\theta$ , noise  $\sigma^2$ , tempering  $\alpha \in (0, 1]$ .

- 1: Build  $K_t$  with  $(K_t)_{ij} = k_\theta(x_i, x_j)$ ; set  $m_t = (m(x_1), \dots, m(x_t))^\top$ .
- 2:  $\Lambda_t(\alpha) \leftarrow K_t + \frac{\sigma^2}{\alpha} I_t$ ; compute Cholesky  $L$  s.t.  $LL^\top = \Lambda_t(\alpha)$ .
- 3: For any vector  $b$ , implement  $\Lambda_t(\alpha)^{-1}b$  via solves  $Lu = b$ ,  $L^T v = u$ .
- 4: **return** functions

$$\mu_{t,\alpha}(x) = m(x) + k_t(x)^T \Lambda_t(\alpha)^{-1} (y_{1:t} - m_t), \quad \sigma_{t,\alpha}^2(x) = k_\theta(x, x) - k_t(x)^T \Lambda_t(\alpha)^{-1} k_t(x).$$


---

---

**Algorithm 4** GEI( $\mu, \sigma, \mu^+, g$ )

---

**Require:** Predictive mean  $\mu$ , std. dev.  $\sigma > 0$ , threshold  $\mu^+$ , integer  $g \geq 0$ .

- 1: **If**  $\sigma = 0$  **then return** 0.
- 2:  $v \leftarrow (\mu^+ - \mu)/\sigma$  ▷ Standardized gap (nonnegative when  $\mu \leq \mu^+$ )
- 3: **If**  $g = 0$  **then return**  $\Phi(-v)$ .
- 4: **If**  $g = 1$  **then return**  $\sigma(\varphi(v) - v\Phi(-v))$  ▷ Classic EI
- 5: Compute  $\tau_g(v)$  via TAU<sup>SERIES</sup>( $v, g$ ) (Alg. 5).
- 6: **return**  $\sigma^g \tau_g(v)$ .

---



---

**Algorithm 5** TAU<sup>SERIES</sup>( $v, g$ ): compute  $\tau_g(v) = \sum_{k=0}^g (-1)^k \binom{g}{k} v^k T_{g-k}(v)$ 


---

**Require:**  $v \in [0, \infty)$ , integer  $g \geq 0$ .

- 1: Define  $T_0(z) = \Phi(-z)$ ,  $T_1(z) = \varphi(z)$ .
- 2: **for**  $m = 2, 3, \dots, g$  **do**
- 3:      $T_m(z) \leftarrow z^{m-1} \varphi(z) + (m-1)T_{m-2}(z)$  ▷ Define symbolically for current  $z$
- 4: **end for**
- 5:  $\tau \leftarrow 0$
- 6: **for**  $k = 0$  **to**  $g$  **do**
- 7:      $\tau \leftarrow \tau + (-1)^k \binom{g}{k} v^k T_{g-k}(v)$
- 8: **end for**
- 9: **return**  $\tau$

---



---

**Algorithm 6** TEMPERSCHEDELE( $\mathcal{D}_t$ ) (examples)

---

**Require:** Data  $\mathcal{D}_t$ .

- 1: **Option A (fixed):** **return**  $\alpha_t \leftarrow 1$ .
- 2: **Option B (information-matching):** See Section 5 and the update in Equation (10).
- 3: **Option C (conservatism cap):** Choose  $\alpha_t$  as the largest value in  $(0, 1]$  that satisfies a given conservatism constraint (e.g., on an optimism slope proxy or credible width).

---

- (i) For numerical stability, compute  $\Lambda_t(\alpha)^{-1}$  via Cholesky solves; add a small jitter if needed.
- (ii) The series for  $\tau_g$  uses stable building blocks  $T_m$ ; the recursion  $T_m(z) = z^{m-1} \varphi(z) +$

$(m-1)T_{m-2}(z)$  avoids repeated integration.

(iii) Choosing  $g$  controls exploitation–exploration:  $g=0$  is PI,  $g=1$  is classic EI, larger  $g$  emphasizes larger improvements.

## F Proof of GP Regret Bounds

### F.1 Proof of Proposition 4.1

*Proof.* For the integer case  $g$ , the formula closely aligns with (Schonlau et al., 1998), but is derived for finding the global maximum. Define  $u := \frac{f(x) - \mu_{t,\alpha}(x;\theta)}{\sigma_{t,\alpha}(x;\theta)}$ . Note the acquisition function can be reformulated as follows:

$$\alpha_{\theta,g}^{EI(f)} = \begin{cases} \sigma_{t,\alpha}^g(x;\theta)(u-v)^g & \text{if } u > v \\ 0 & \text{otherwise.} \end{cases}$$

Rewriting the acquisition above yields

$$\alpha_{\theta,g,\alpha}^{EI(f)}(x \mid \mathcal{D}_t) = \sigma_{t,\alpha}^g(x;\theta) \tau_g(v_\alpha), \quad \tau_g(v) := \int_v^\infty (u-v)^g \phi(u) du. \quad (18)$$

To show that the function  $\tau_g(\cdot)$  has closed-form expression for the integer  $g$ , observe that the the sole randomness of  $\alpha_{\theta,g}^{EI(f)}$  comes from  $u$ . Hence we have

$$\begin{aligned} \alpha_{\theta,g,\alpha}^{EI(f)} &= \sigma_{t,\alpha}^g(x;\theta) \int_v^\infty \sum_{k=0}^g (-1)^k \binom{g}{k} u^{g-k} v^k \phi(u) du \\ &= \sigma_{t,\alpha}^g(x;\theta) \left\{ \sum_{k=0}^g (-1)^k \binom{g}{k} v^k \int_v^\infty u^{g-k} \phi(u) du \right\} \\ &= \sigma_{t,\alpha}^g(x;\theta) \left\{ \sum_{k=0}^g (-1)^k \binom{g}{k} v^k T_{g-k} \right\}, \end{aligned}$$

where we define  $T_m := \int_v^\infty u^m \phi(u) du$ . To show the recursive relationship, note  $T_m$  can be computed explicitly through integration by part by writing  $u^m = u^{m-1}u$ . This shows

$$T_m = [-u^{m-1} \phi(u)]_v^\infty - \int_v^\infty (-\phi(u))(m-1)u^{m-2} du = v^{m-1} \phi(v) + (m-1)T_{m-2}.$$

Additionally, it is easy to compute the base cases

$$\begin{aligned} T_0 &= \int_v^\infty \phi(u) du = 1 - \Phi(v) = \Phi(-v), \\ T_1 &= \int_v^\infty u \phi(u) du = [-\phi(u)]_v^\infty = \phi(v). \end{aligned}$$

As an additional remark, we may also derive a series representation of the general  $g$  case similarly, except that we need to express  $(u-v)^g$  via a infinite series using the generalized

binomial theorem. Specifically, we have

$$\begin{aligned}
\alpha_{\theta,g,\alpha}^{EI(f)} &= \sigma_{t,\alpha}^g(x; \theta) \int_v^\infty (u - v)^g \phi(u) du \\
&= \sigma_{t,\alpha}^g(x; \theta) \int_v^\infty u^g \left\{ \sum_{k=0}^{\infty} \binom{g}{k} (-1)^k \left(\frac{v}{u}\right)^k \right\} \phi(u) du \\
&= \sigma_{t,\alpha}^g(x; \theta) \left\{ \sum_{k=0}^{\infty} (-1)^k \binom{g}{k} v^k \int_v^\infty u^{g-k} \phi(u) du \right\} \\
&= \sigma_{t,\alpha}^g(x; \theta) \left\{ \sum_{k=0}^{\infty} (-1)^k \binom{g}{k} v^k T_{g-k} \right\}.
\end{aligned}$$

□

We study the properties of  $\tau_g(\cdot)$  for the integer case in Lemma F.1 and the general positive real case in Lemma F.2.

## F.2 Analysis of $\tau_g$

**Lemma F.1.** *For  $g \in \mathcal{N}^+$ , consider the function*

$$\tau_g(z) := \sum_{k=0}^g (-1)^k \binom{g}{k} z^k T_{g-k}(z), \quad (19)$$

where  $T_0(z) = \Phi(-z)$ ,  $T_1(z) = \phi(z)$ , and  $T_m(z) = z^{m-1}\phi(z) + (m-1)T_{m-2}(z)$  for  $m > 1$ . The function  $\tau_g(\cdot)$  has the following properties:

1.  $T'_m(z) = -z^m \phi(z)$ .
2.  $\tau_g(z)$  is a decreasing function in  $z$  for any fixed  $g \in \mathcal{N}^+$ .
3. For  $z \leq 0$ ,  $\tau_g(z) \leq (g-1)!!(1+|z|)^g$  for any  $g \in \mathcal{N}^+$ , where  $(g-1)!! := (g-1) \times (g-3) \times \dots$ , and  $1!! = 0!! = 1$ .
4. For  $u_0 := \min\left\{1, -\frac{z}{2}\right\} > 0$ , the following *positive* lower bound holds:

$$\tau_g(z) \geq \frac{u_0^{g+1}}{g+1} \phi(z + u_0), \quad z \leq 0. \quad (20)$$

In particular

$$-2 < z \leq 0 : \quad \tau_g(z) \geq \frac{(-z)^{g+1}}{2^{g+1}(g+1)} \phi\left(\frac{z}{2}\right), \quad (21)$$

$$z \leq -2 : \quad \tau_g(z) \geq \frac{1}{g+1} \phi(z+1). \quad (22)$$

*Proof.* 1. We can see this by induction. To establish the base case, note that Since  $T_0(z) = \Phi(-z)$  and  $T_1(z) = \phi(z)$ , we have  $T'_0(z) = -\phi(z)$  and  $T'_1(z) = \phi'(z) = -z\phi(z)$ . Suppose this pattern holds for any integer less than  $k$ . Since  $T_m(z) = z^{m-1}\phi(z) + (m-1)T_{m-2}(z)$ , we have

$$\begin{aligned} T'_{k+1}(z) &= kz^{k-1}\phi(z) + z^k\phi'(z) + kT'_{k-1}(z) \\ &= kz^{k-1}\phi(z) - z^{k+1}\phi(z) - kz^{k-1}\phi(z) \\ &= -z^{k+1}\phi(z). \end{aligned}$$

2. By the product rule, we can decompose the derivative of  $\tau_g$  into two parts:

$$\tau'_g(z) = \sum_{k=0}^g (-1)^k \binom{g}{k} kz^{k-1} T_{g-k}(z) + \sum_{k=0}^g (-1)^k \binom{g}{k} kz^k T'_{g-k}(z)$$

The first summation can be computed as follows:

$$\begin{aligned} \sum_{k=0}^g (-1)^k \binom{g}{k} kz^{k-1} T_{g-k}(z) &= \sum_{k'=0}^{g-1} (-1)^{k'+1} \binom{g}{k'+1} (k'+1) z^{k'} T_{g-(k'+1)}(z) \\ &= \sum_{k'=0}^{g-1} (-1)^{k'+1} g \binom{g-1}{k'} z^{k'} T_{g-(k'+1)}(z) \\ &= -g \sum_{k=0}^{g-1} (-1)^{k'} \binom{g-1}{k'} z^{k'} T_{g-(k'+1)}(z) \\ &= -g\tau_{g-1}(z). \end{aligned}$$

It is also possible to show the second summation is zero by the first part of the lemma:

$$\begin{aligned} \sum_{k=0}^g (-1)^k \binom{g}{k} kz^k T'_{g-k}(z) &= \sum_{k=0}^g (-1)^k \binom{g}{k} kz^k (-z^{g-k}\phi(z)) \\ &= -\phi(z) z^g \sum_{k=0}^g \sum_{k=0}^g (-1)^k \binom{g}{k} \\ &= -\phi(z) z^g (1-1)^g = 0. \end{aligned}$$

Hence we have  $\tau'_g(z) = -g\tau_{g-1}(z)$ . Since the generalized expected improvement  $\alpha_{\theta,g}^{EI(f)}(x|\mathcal{D}_t)$  is always positive, hence  $\tau'_g(z) = -g\tau_{g-1}(z) < 0$ .

3. Since  $z \leq 0$  and  $T'_m(z) = -z^m\phi(z)$ , we know the function  $T_m(z)$  is increasing in  $z$  for odd  $m$  but decreasing in  $z$  for even  $m$ . When  $m$  is odd and  $z \leq 0$ , we have  $T_m(z) \leq T_m(0) = (m-1)!!\phi(0)$ . Similarly, when  $m$  is even and  $z < 0$ , we have

$$T_m(z) = z^{m-1}\phi(z) + (m-1)T_{m-2}(z) \leq (m-1)T_{m-2}(z) \leq (m-1)!!\Phi(-z).$$

Hence we have  $T_m(z) \leq (m-1)!!$  for any  $z \leq 0$ . It follows

$$\tau_g(z) \leq \sum_{k=0}^g (-1)^k \binom{g}{k} z^k (g-k-1)!! \leq (g-1)!! (1+|z|)^g.$$

4. Recall that

$$T_m(z) = \int_z^\infty u^m \phi(u) du, \quad m \geq 0.$$

Define the moment polynomial

$$\tau_g(z) = \sum_{k=0}^g \binom{g}{k} (-1)^k z^k T_{g-k}(z).$$

These two definitions gives

$$\tau_g(z) = \int_0^\infty u^g \phi(z+u) du, \quad z \leq 0.$$

Using  $u_0 := \min\left\{1, -\frac{z}{2}\right\} > 0$  defined above,  $\tau_g(z) \geq \int_0^{u_0} u^g \phi(z+u) du$ . Because  $u \in [0, u_0]$  and  $z \leq 0$ ,  $z \leq z+u \leq z+u_0 \leq 0$ . The Gaussian pdf is increasing on  $(-\infty, 0]$ , therefore

$$\phi(z+u) \geq \phi(z+u_0) \quad \text{for } u \in [0, u_0]. \quad (23)$$

$$\int_0^{u_0} u^g du = \frac{u_0^{g+1}}{g+1}. \quad (24)$$

Now we can multiply the (23) and (24) yields (20).

- (a) If  $-2 < z \leq 0$ , then  $u_0 = -z/2$  and (21) follows.
- (b) If  $z \leq -2$ , then  $u_0 = 1$  and (22) follows.

□

**Lemma F.2.** For  $g \in \mathcal{R}^+$ , consider the function

$$\tau_g(z) := \int_z^\infty (u-z)^g \phi(u) du = \sum_{k=0}^\infty (-1)^k \binom{g}{k} z^k T_{g-k}(z), \quad (25)$$

where  $T_m(z) := \int_z^\infty u^m \phi(u) du$ . The function  $\tau_g(\cdot)$  has the following properties:

- (I)  $T'_m(z) = -z^m \phi(z)$ .
- (II)  $\tau_g(z)$  is a decreasing function in  $z$  for any fixed  $g \geq 0$ .
- (III) For  $z \geq 0$ ,  $\tau_g(z) \leq \frac{2^{g/2-1} \Gamma((g+1)/2)}{\sqrt{\pi}}$  for any  $g \geq 0$ .

*Proof.* (I) By direct application of the Leibniz rule for differentiation, we have

$$\begin{aligned}\frac{d}{dz} \int_z^\infty u^m \phi(u) du &= \lim_{u \rightarrow \infty} u^m \phi(u) \cdot 0 - z^m \phi(z) \cdot 1 \\ &= -z^m \phi(z).\end{aligned}$$

(II) Differentiate the integral form (Leibniz + chain rule):

$$\frac{d}{dz} \tau_g(z) = \frac{d}{dz} \int_z^\infty (u-z)^g \phi(u) du \quad (26)$$

$$= \int_z^\infty \frac{\partial}{\partial z} (u-z)^g \phi(u) du \quad (27)$$

$$= -g \int_z^\infty (u-z)^{g-1} \phi(u) du \quad (28)$$

$$= -g \tau_{g-1}(z). \quad (29)$$

Hence we have

$$\tau'_g(z) = -g \tau_{g-1}(z) \quad (g > 0).$$

Note  $\tau_0(z) = 1 - \Phi(z)$ , which is obviously a decreasing function.

(III) Since  $\tau_g(z)$  is decreasing function in  $z$ . It is sufficient to show  $\tau_g(0) = \frac{2^{g/2-1} \Gamma((g+1)/2)}{\sqrt{\pi}}$ .  
Following the proof in Proposition 4.1, we have

$$\begin{aligned}\tau_g(0) &= \int_0^\infty u^g \phi(u) du = \frac{1}{\sqrt{2\pi}} \int_0^\infty u^g e^{-u^2/2} du \\ &= \frac{1}{\sqrt{2\pi}} \int_0^\infty (2t)^{\frac{g}{2}} e^{-t} \frac{\sqrt{2}}{2\sqrt{t}} dt \\ &= \frac{1}{\sqrt{2\pi}} 2^{(g-1)/2} \int_0^\infty t^{(g-1)/2} e^{-t} dt \\ &= \frac{2^{g/2-1} \Gamma((g+1)/2)}{\sqrt{\pi}}.\end{aligned}$$

□

### F.3 Concentration Result of Tempered Posterior

We derive the concentration bound for GP alpha posterior.

**Lemma F.3.** *For any  $\eta > 0$ , we have*

$$P(-\epsilon_T^T (K_T + \frac{\sigma^2}{\alpha} \mathbb{I})^{-1} \epsilon_T + \alpha \sigma^{-2} \|\epsilon_T\|^2 > 2\alpha \gamma_{T,\alpha}^\theta + 2\alpha \sqrt{2\gamma_{T,\alpha}^\theta \eta} + 2\alpha \eta) \leq e^{-\eta}.$$

*Proof.* This proof follows an analogy of Lemma 4 in (Wang and de Freitas, 2014). We present our proof of the  $\alpha$ -posterior version for the completeness of our presentation. Define  $\Lambda := \alpha \sigma^{-2} \mathbb{I} - (K_T^\theta + \frac{\sigma^2}{\alpha} \mathbb{I})^{-1}$ . Then we have  $-\epsilon_T^T (K_T + \frac{\sigma^2}{\alpha} \mathbb{I})^{-1} \epsilon_T + \alpha \sigma^{-2} \|\epsilon_T\|^2 := \epsilon_T^T \Lambda \epsilon_T$ . Let

$Q^T \Sigma Q$  be the eigendecomposition of  $\Lambda$  and  $\Delta_i$  be the  $i$ -th eigen value of  $K_T^\theta$ . It is easy to check the diagonal element of  $\Sigma$  has the form

$$\Sigma_{ii} = \frac{\alpha}{\sigma^2} - \frac{1}{\Delta_i + \sigma^2/\alpha} = \frac{\alpha^2 \Delta_i}{\sigma^2(\alpha \Delta_i + \sigma^2)}.$$

It follows

$$\begin{aligned} \text{tr}(\Lambda) &= \text{tr}(\Sigma) = \sum_{i=1}^T \frac{\alpha^2 \Delta_i}{\sigma^2(\alpha \Delta_i + \sigma^2)} = \frac{\alpha}{\sigma^2} \sum_{t=1}^T \frac{\alpha \Delta_i / \sigma^2}{\alpha \Delta_i / \sigma^2 + 1} \leq \frac{\alpha}{\sigma^2} \sum_{t=1}^T \log\left(1 + \frac{\alpha \Delta_i}{\sigma^2}\right). \\ \text{tr}(\Lambda^2) &= \text{tr}(\Sigma^2) = \sum_{i=1}^T \left(\frac{\alpha^2 \Delta_i}{\sigma^2(\alpha \Delta_i + \sigma^2)}\right)^2 \leq \frac{\alpha^2}{\sigma^2} \sum_{i=1}^T \frac{\alpha^2 \Delta_i}{\sigma^2(\alpha \Delta_i + \sigma^2)} \leq \frac{\alpha^2}{\sigma^4} \sum_{t=1}^T \log\left(1 + \frac{\alpha \Delta_i}{\sigma^2}\right). \\ \|\Lambda\|_2 &= \max_{i \leq T} \frac{\alpha^2 \Delta_i}{\sigma^2(\alpha \Delta_i + \sigma^2)} \leq \frac{\alpha}{\sigma^2}. \end{aligned}$$

By the definition of  $\gamma_{T,\alpha}^\theta$ , we have

$$\text{tr}(\Lambda) \leq 2\alpha\sigma^{-2}\gamma_{T,\alpha}^\theta, \quad \text{tr}(\Lambda^2) \leq 2\alpha^2\sigma^{-4}\gamma_{T,\alpha}^\theta.$$

By a version of Hanson-Wright concentration inequality presented by Theorem 2.1 of (Hsu et al., 2012), we have

$$\begin{aligned} P(\epsilon_T^T \Lambda \epsilon_T > \sigma^2 \{2\alpha\sigma^{-2}\gamma_{T,\alpha}^\theta + 2\sqrt{2\alpha^2\sigma^{-4}\gamma_{T,\alpha}^\theta \eta} + 2\alpha\sigma^{-2}\eta\}) \\ &\leq P(\epsilon_T^T \Lambda \epsilon_T > \sigma^2(\text{tr}(\Delta) + 2\sqrt{\text{tr}(\Delta^2)\eta} + 2\|\Lambda\|_2\eta)) \\ &\leq e^{-\eta}. \end{aligned}$$

□

We need the following concentration result for the  $\alpha$ -posterior:

**Theorem F.4.** *We have the concentration inequality:*

$$\mathbb{P}(\|\mu_{T,\alpha}(\cdot; \theta) - f(\cdot)\|_{\mathcal{K}_{T,\alpha}} \leq \varphi_{T+1,\alpha}^\theta) \geq 1 - \frac{6\delta}{\pi^2(T+1)^2},$$

where we define

$$\begin{aligned} (\varphi_{T,\alpha}^\theta)^2 &= \|f\|_{\mathcal{H}_\theta(\mathcal{X})}^2 + \alpha \sqrt{8\gamma_{T-1,\alpha}^\theta \log\left(\frac{2T^2\pi^2}{3\delta}\right)} + \sqrt{8\alpha \log\left(\frac{2T^2\pi^2}{3\delta}\right)} \|f\|_{\mathcal{H}_\theta(\mathcal{X})} + \\ &\quad 2\alpha\gamma_{T-1,\alpha}^\theta + 2\alpha \log\left(\frac{T^2\pi^2}{3\delta}\right). \end{aligned} \quad (30)$$

*Proof.* It is straightforward to verify that the RKHS norm for a function  $f$  corresponding to  $\mathcal{K}_{T,\alpha}$  is given by  $\|f\|_{\mathcal{K}_{T,\alpha}}^2 = \|f\|_{K_T}^2 + \alpha\sigma^{-2} \sum_{t \leq T} f(x_t)^2$  under the  $\alpha$ -posterior. Hence we

have

$$\|\mu_{T,\alpha}(\cdot; \theta) - f(\cdot)\|_{\mathcal{K}_{T,\alpha}}^2 = \|\mu_{T,\alpha} - f\|_{\mathcal{H}_\theta(\mathcal{X})}^2 + \alpha\sigma^{-2} \sum_{t \leq T} (\mu_{T,\alpha}(x, T) - f(x_t))^2.$$

Following a similar notation as in Lemma 7.2 of (Srinivas et al., 2012), we define  $\mathbf{b}_t := (K_T + \frac{\sigma^2}{\alpha} \mathbb{I})^{-1} y_T$ . It is easy to see  $\mu_{t,\alpha}(x) = \mathbf{b}_t^T k_t(x)$ ,  $\langle \mu_{T,\alpha}, f \rangle_{\mathcal{H}_\theta(\mathcal{X})} = f_T^T \mathbf{b}_T$ , and  $y_T = K_T \mathbf{b}_T + \frac{\sigma^2}{\alpha} \mathbf{b}_T$ . Since  $\|\mu_{t,\alpha}\|_{\mathcal{H}_\theta(\mathcal{X})}^2 = \mathbf{b}_T^T K_T \mathbf{b}_T$ , and  $y_T^T \mathbf{b}_T = \mathbf{b}_T^T K_T \mathbf{b}_T + \frac{\sigma^2}{\alpha} \|\mathbf{b}_T\|^2$ , we know  $\|\mu_{T,\alpha}\|_k^2 = y_T^T \mathbf{b}_T - \frac{\sigma^2}{\alpha} \|\mathbf{b}_T\|^2$ . This allows us to rewrite the expression as follows:

$$\begin{aligned} \|\mu_{T,\alpha}(\cdot; \theta) - f(\cdot)\|_{\mathcal{K}_{T,\alpha}}^2 &= \|f\|_{\mathcal{H}_\theta(\mathcal{X})}^2 + \|\mu_{T,\alpha}(\cdot, \theta)\|_{\mathcal{H}_\theta(\mathcal{X})}^2 - 2\langle \mu_{T,\alpha}, f \rangle_{\mathcal{H}_\theta(\mathcal{X})} \\ &\quad + \alpha\sigma^{-2} \sum_{t \leq T} ((y_t - \frac{\sigma^2}{\alpha} b_t) - (y_t - \epsilon_t))^2 \\ &= \|f\|_{\mathcal{H}_\theta(\mathcal{X})}^2 - y_T^T \mathbf{b}_T + \alpha\sigma^{-2} \|\epsilon_T\|^2 \\ &= \|f\|_{\mathcal{H}_\theta(\mathcal{X})}^2 - y_T^T (K_T + \frac{\sigma^2}{\alpha} \mathbb{I})^{-1} y_T + \alpha\sigma^{-2} \|\epsilon_T\|^2 \\ &= \|f\|_{\mathcal{H}_\theta(\mathcal{X})}^2 - f_T^T (K_T + \frac{\sigma^2}{\alpha} \mathbb{I})^{-1} f_T - 2f_T^T (K_T + \frac{\sigma^2}{\alpha} \mathbb{I})^{-1} \epsilon_T \\ &\quad - \epsilon_T^T (K_T + \frac{\sigma^2}{\alpha} \mathbb{I})^{-1} \epsilon_T + \alpha\sigma^{-2} \|\epsilon_T\|^2 \\ &\leq \|f\|_{\mathcal{H}_\theta(\mathcal{X})}^2 - 2f_T^T (K_T + \frac{\sigma^2}{\alpha} \mathbb{I})^{-1} \epsilon_T - \epsilon_T^T (K_T + \frac{\sigma^2}{\alpha} \mathbb{I})^{-1} \epsilon_T + \alpha\sigma^{-2} \|\epsilon_T\|^2. \end{aligned}$$

First observe that  $f_T^T (K_T + \frac{\sigma^2}{\alpha} \mathbb{I})^{-1} \epsilon_T$  is  $\sqrt{\alpha} \|f\|_{\mathcal{H}_\theta(\mathcal{X})}$  sub-gaussian since

$$\begin{aligned} f_T^T (K_T + \frac{\sigma^2}{\alpha} \mathbb{I})^{-1} (K_T + \frac{\sigma^2}{\alpha} \mathbb{I})^{-1} f_T &= \text{tr}(f_T^T (K_T + \frac{\sigma^2}{\alpha} \mathbb{I})^{-2} f_T) \\ &\leq \frac{\alpha}{\sigma^2} \text{tr}(f_T^T (K_T + \frac{\alpha}{\sigma^2} \mathbb{I})^{-1} f_T) \leq \frac{\alpha}{\sigma^2} \|f\|_{\mathcal{H}_\theta(\mathcal{X})}^2. \end{aligned}$$

It follows that  $2f_T^T (K_T + \frac{\sigma^2}{\alpha} \mathbb{I})^{-1} \epsilon_T$  is  $2\sqrt{\alpha} \|f\|_{\mathcal{H}_\theta(\mathcal{X})}$  sub-gaussian. By standard concentration result for sub-gaussian random variable, we have

$$P(2f_T^T (K_T + \frac{\sigma^2}{\alpha} \mathbb{I})^{-1} \epsilon_T \geq \sqrt{8\alpha \log\left(\frac{2T^2\pi^2}{3\delta}\right)} \|f\|_{\mathcal{H}_\theta(\mathcal{X})}) \leq \frac{3\delta}{(T+1)^2\pi^2}.$$

Additionally With  $\eta = \log(\frac{(T+1)^2\pi^2}{3\delta})$ , a direct application of lemma F.3 yields

$$\begin{aligned} P(-\epsilon_T^T (K_T + \frac{\sigma^2}{\alpha} \mathbb{I})^{-1} \epsilon_T + \alpha\sigma^{-2} \|\epsilon_T\|^2 \geq \alpha \sqrt{8\gamma_{T-1,\alpha}^\theta \log\left(\frac{2T^2\pi^2}{3\delta}\right)} + 2\alpha\gamma_{T-1,\alpha}^\theta + 2\alpha \log\left(\frac{T^2\pi^2}{3\delta}\right)) \\ \leq \frac{3\delta}{2\pi^2(T+1)^2}. \end{aligned}$$

Hence we have

$$\mathbb{P}(\|\mu_{T,\alpha}(\cdot; \theta) - f(\cdot)\|_{\mathcal{K}_{T,\alpha}} \leq \varphi_{T+1,\alpha}^\theta) \geq 1 - \frac{6\delta}{\pi^2(T+1)^2}.$$

□

## F.4 Auxiliary Lemmas

**Lemma F.5.** *Assuming  $|\mu_{t-1,\alpha}(x, \theta_t) - f(x)| \leq \varphi_{t,\alpha}^{\theta_t} \sigma_{t-1,\alpha}(x; \theta_t)$ , then*

$$\mu_\theta^+ - \mu_{t-1,\alpha}(x_t) \leq \tau_g^{-1} \left( \frac{\Gamma(\frac{g+1}{2})}{2\sqrt{\pi}} \left( \frac{2\sigma^2}{\alpha(t-1) + \sigma^2} \right)^{g/2} \right) \nu \sigma_{t-1,\alpha}(x_t; \theta_t) \quad (31)$$

*Proof.* We define  $x_t^+ = \arg \max_{x \in \mathcal{X}} \mu_{t-1,\alpha}(x; \theta_t)$ . Since  $\alpha_{\theta,g,\alpha}^{EI(f)}(x_t | \mathcal{D}_{t-1}) \geq \alpha_{\theta,g,\alpha}^{EI(f)}(x^+ | \mathcal{D}_{t-1})$ , we have

$$\nu^g \sigma_{t-1,\alpha}^g(x_t; \theta) \tau_g \left( \frac{\mu_{\theta,\alpha}^+ - \mu_{t-1,\alpha}(x_t)}{\nu \sigma_{t-1,\alpha}(x_t; \theta)} \right) \geq \nu^g \sigma_{t-1,\alpha}^g(x_t^+; \theta) \tau_g(0)$$

We start by finding a lower bound for the right hand side of the inequality above. First observe that using the same step as in part (III) of Lemma F.2, we have  $\tau_g(0) = \frac{2^{g/2-1} \Gamma((g+1)/2)}{\sqrt{\pi}}$ . By the same argument as in Lemma 10 of Wang and de Freitas (2014), we have  $\sigma_{t-1}^2(x_t^+; \theta_t) \geq \frac{\sigma^2}{\alpha(t-1) + \sigma^2}$ , since

$$\sigma_{t-1,\alpha}^2(x_t^+; \theta_t) \geq 1 - \mathbf{1}^T (\mathbf{1} \mathbf{1}^T + \frac{\sigma^2}{\alpha} \mathbb{I})^{-1} \mathbf{1} = 1 - \frac{\|\mathbf{1}\|_2^2}{\|\mathbf{1}\|_2^2 + \sigma^2/\alpha} = \frac{\sigma^2}{\alpha(t-1) + \sigma^2}.$$

The lower bound above holds since we can bound the posterior variance at  $x_t^+$  in the extreme case where all  $(t-1)$  observations are collected at the same point. Since  $\sigma_{t-1,\alpha}^g(x_t; \theta) \leq 1$  is still bounded by the prior variance  $k(x, x)$ , it follows

$$\frac{\Gamma(\frac{g+1}{2})}{2\sqrt{\pi}} \left( \frac{2\sigma^2}{\alpha(t-1) + \sigma^2} \right)^{g/2} \leq \tau_g \left( \frac{\mu_\theta^+ - \mu_{t-1}(x_t)}{\nu \sigma_{t-1}(x_t; \theta)} \right).$$

Since  $\tau_g(\cdot)$  is a decreasing function by Lemma F.2 and its inverse is well-defined, we must have

$$\mu_\theta^+ - \mu_{t-1,\alpha}(x_t) \leq \tau_g^{-1} \left( \frac{\Gamma(\frac{g+1}{2})}{2\sqrt{\pi}} \left( \frac{2\sigma^2}{\alpha(t-1) + \sigma^2} \right)^{g/2} \right) \nu \sigma_{t-1}(x_t; \theta_t).$$

□

## F.5 Proof of Theorem 4.2

*Proof.* Define  $\mu_{\theta_t,\alpha}^+ := \max_{x \in \mathcal{X}} \mu_{t-1,\alpha}(x; \theta_t)$ , and  $x_t := \arg \max_{x \in \mathcal{X}} \alpha_{\theta,g,\alpha}^{EI(f)}(x | \mathcal{D}_{t-1})$ . We further define the random variable

$$I_{t,g,\alpha}^\theta = (\max\{0, f(x) - \mu_{\theta_t,\alpha}^+\})^g.$$

We have the instantaneous regret

$$\begin{aligned} r_t &= f(x^*) - f(x_t) = [f(x^*) - \mu_{\theta_t, \alpha}^+] - [f(x_t) - \mu_{\theta_t, \alpha}^+] \\ &\leq I_{t,1,\alpha}^\theta(x^*) - [f(x_t) - \mu_{\theta_t, \alpha}^+]. \end{aligned}$$

By Cauchy-Schwarz and the choice of  $\varphi_{t,\alpha}^{\theta_t}$  as presented in Theorem F.4, we have

$$\begin{aligned} |\mu_{t-1,\alpha}(\mathbf{x}, \theta_t) - f(\mathbf{x})| &\leq (\mathcal{K}_{t-1,\alpha}^{\theta_t}(\mathbf{x}, \mathbf{x}))^{1/2} \|\mu_{t-1}(\cdot; \theta_t) - f(\cdot)\|_{\mathcal{K}_{t-1}^{\theta_t}} \\ &= \sigma_{t-1,\alpha}(\mathbf{x}; \theta_t) \|\mu_{t-1,\alpha}(\cdot; \theta_t) - f(\cdot)\|_{\mathcal{K}_{t-1}^{\theta_t}} \\ &\leq \sigma_{t-1,\alpha}(x; \theta_t) \varphi_{t,\alpha}^{\theta_t}, \quad \text{w.p. } 1 - \frac{6\delta}{\pi^2 t^2}. \end{aligned}$$

Hence by the union bound, with probability at least  $1 - \delta$ , we have

$$|\mu_{t-1,\alpha}(\mathbf{x}, \theta_t) - f(\mathbf{x})| \leq \varphi_{t,\alpha}^{\theta_t} \sigma_{t-1,\alpha}(x; \theta_t), \quad \forall t \in \mathcal{N}, x \in \mathcal{X}.$$

This suggests  $f(x_t) \geq \mu_{t-1,\alpha}(x; \theta_t) - \varphi_{t,\alpha}^{\theta_t} \sigma_{t-1,\alpha}(x_t; \theta_t)$ . Hence the instantaneous regret can be further upper bounded by:

$$r_t \leq I_{t,1,\alpha}^\theta(x^*) + [\varphi_{t,\alpha}^{\theta_t} \sigma_{t-1}(x_t; \theta_t) + (\mu_{\theta_t, \alpha}^+ - \mu_{t-1,\alpha}(x_t; \theta_t))].$$

To upper bound  $I_{t,1,\alpha}^\theta(x^*)$ , we apply same argument as in Lemma 9 of (Wang and de Freitas, 2014)<sup>2</sup>, and we obtain

$$I_{t,1,\alpha}^\theta(x^*) \leq \frac{\tau_1(-\varphi_{t,\alpha}^{\theta_t}/\nu_{\theta_t})}{\tau_1(\varphi_{t,\alpha}^{\theta_t}/\nu_{\theta_t})} \alpha_{\theta_t,1,\alpha}^{\text{EI}}(x^* | D_{t-1}).$$

To see why the last inequality is true, observe that  $\varphi_{t,\alpha}^{\theta_t}$  increases with  $\alpha$  as the maximum information gain  $\gamma_{t,\alpha}$  increases with  $\alpha$ , and  $\tau_1(\cdot)$  is a strictly decreasing function by Lemma F.2. Our choice of  $\nu_t$  makes sure the ratio of  $\frac{\varphi_{t,\alpha}^{\theta_t}}{\nu_{\theta_t}} \leq C_4$  is uniformly bounded for some constant  $C_4$ . Hence there exists a constant  $C_3$  (unrelated to  $\alpha$ ) such that  $I_{t,1,\alpha}^\theta \leq C_3 \alpha_{\theta_t,1,\alpha}^{\text{EI}}(x^* | D_{t-1})$ . Define constant  $C_{(g)} := \frac{2^{g/2} \Gamma((g+1)/2)}{2\sqrt{\pi}}$ . By the Jensen inequality, and part (III) of Lemma F.2, we have

$$I_{t,1}^\theta(x^*) \leq C_3 (\alpha_{\theta,g,\alpha}^{\text{EI}(f)}(x^* | D_{t-1}))^{1/g} \leq C_3 (\alpha_{\theta,g,\alpha}^{\text{EI}(f)}(x_t | D_{t-1}))^{1/g} \leq C_3 C_{(g)}^{1/g} \nu_{\theta_t} \sigma_{t-1,\alpha}(x_t; \theta) \quad (32)$$

To bound  $(\mu_{\theta_t, \alpha}^+ - \mu_{t-1,\alpha}(x_t; \theta_t))$ , we apply lemma F.5, which yields

$$(\mu_{\theta_t, \alpha}^+ - \mu_{t-1,\alpha}(x_t; \theta_t)) \leq \tau_g^{-1} \left( \frac{\Gamma(\frac{g+1}{2})}{2\sqrt{\pi}} \left( \frac{2\sigma^2}{\alpha(t-1) + \sigma^2} \right)^{g/2} \right) \nu_{\theta_t} \sigma_{t-1,\alpha}(x_t; \theta_t).$$

---

<sup>2</sup>Note the authors of (Wang and de Freitas, 2014) defines function  $\tau(z) := z\Phi(z) + \phi(z)$ , which is equivalent to  $\tau_1(-z)$  defined in our paper. By equation (19), we have  $\tau_1(z) = \phi(z) - z\Phi(-z)$ .

By combining the inequalities above, we can upper bound the simple regret as follows:

$$\begin{aligned}
r_t &\leq C_3 C_{(g)}^{1/g} \nu_{\theta_t} \sigma_{t-1,\alpha}(x_t; \theta) + \varphi_{t,\alpha}^{\theta_t} \sigma_{t-1,\alpha}(x_t; \theta_t) \\
&\quad + \tau_g^{-1} \left( \frac{\Gamma(\frac{g+1}{2})}{2\sqrt{\pi}} \left( \frac{2\sigma^2}{\alpha(t-1) + \sigma^2} \right)^{g/2} \right) \nu_{\theta_t}^{\theta_t} \sigma_{t-1,\alpha}(x_t; \theta_t) \\
&= \sigma_{t-1,\alpha}(x_t; \theta_t) \left\{ C_3 C_{(g)}^{1/g} \nu_{\theta_t} + \varphi_{t,\alpha}^{\theta_t} + \tau_g^{-1} \left( C_{(g)} \left( \frac{\sigma^2}{\alpha(t-1) + \sigma^2} \right)^{g/2} \right) \nu_{\theta_t} \right\}
\end{aligned}$$

By lemma 8 of (Wang and de Freitas, 2014), we have  $\|f\|_{\mathcal{H}_\theta}^2 \leq C_2 \|f\|_{\mathcal{H}_{\theta^U}}^2$ . Since  $\gamma_{t,\alpha}^{\theta_t} \leq \gamma_{t,\alpha}^{\theta^L}$ , we have our choice of  $\varphi_{t,\alpha}^L \geq \varphi_{t,\alpha}^{\theta_t}$ . Hence the instantaneous regret can be further bounded as follows:

$$r_t \leq \sigma_{t-1,\alpha}(x_t; \theta_L) \left\{ C_3 C_{(g)}^{1/g} \nu_{\theta_L, t} + \varphi_{t,\alpha}^L + \tau_g^{-1} \left( C_{(g)} \left( \frac{\sigma^2}{\alpha(t-1) + \sigma^2} \right)^{g/2} \right) \nu_{\theta_L, t} \right\}. \quad (33)$$

By the argument in Part (II) of Lemma F.2 and the inverse derivative formula, we may compute the derivative of  $\tau_g^{-1}(z)$  as  $\frac{1}{\tau_g'(z)} = -\frac{1}{g\tau_{g-1}(z)} \leq 0$ . Hence  $\tau_g^{(-1)}(\cdot)$  is monotonically decreasing from  $(0, c_0)$ , where  $c_0 = \tau_g(0) = C_{(g)}$ . since  $(\frac{\sigma^2}{\alpha(t-1) + \sigma^2})^{g/2} < 1$ , we know the inverse function is well-defined for all  $t \geq 1$ . This suggests

$$\begin{aligned}
\sum_t r_t^2 &= \sum_t \sigma_{t-1,\alpha}^2(x_t; \theta^L) \left\{ C_3 C_{(g)}^{1/g} \nu_{\theta_L, t} + \varphi_{t,\alpha}^L + \tau_g^{-1} \left( C_{(g)} \left( \frac{\sigma^2}{\alpha(t-1) + \sigma^2} \right)^{g/2} \right) \nu_{\theta_L, t} \right\}^2 \\
&\leq \sum_t \sigma_{t-1,\alpha}^2(x_t; \theta^L) \left\{ C_3 C_{(g)}^{1/g} \nu_{\theta_L, T} + \varphi_{t,\alpha}^L + \tau_g^{-1} \left( C_{(g)} \left( \frac{\sigma^2}{\alpha(T-1) + \sigma^2} \right)^{g/2} \right) \nu_{\theta_L, T} \right\}^2 \\
&\leq \left( \frac{2}{\alpha \log(1 + \sigma^{-2})} \gamma_{T,\alpha}^{\theta_L} \right) \left\{ C_3 C_{(g)}^{1/g} \nu_{\theta_L, T} + \varphi_{t,\alpha}^L + \tau_g^{-1} \left( C_{(g)} \left( \frac{\sigma^2}{\alpha(T-1) + \sigma^2} \right)^{g/2} \right) \nu_{\theta_L, T} \right\}^2
\end{aligned}$$

To see why the last inequality is true, observe that the function  $\frac{x}{\log(1+x)}$  is increasing, and hence we have  $s^2 \leq \frac{\sigma^{-2}}{\log(1+\sigma^{-2})} \log(1 + s^2)$  for any  $s^2 \in [0, \sigma^{-2}]$ . With the choice of  $s^2 := \alpha\sigma^{-2}\sigma_{t-1,\alpha}^2(x_t) \leq \sigma^{-2}$ ,<sup>3</sup> we have

$$\sum_t \sigma_{t-1,\alpha}^2(x_t; \theta^L) \leq \sum_t \frac{\sigma^2/\alpha}{\sigma^2 \log(1 + \sigma^{-2})} \log(1 + \alpha\sigma^{-2}\sigma_{t-1,\alpha}^2(x_t)) \leq \frac{2}{\alpha \log(1 + \sigma^{-2})} \gamma_{T,\alpha}^{\theta_L}.$$

Finally, by  $R_t^2 \leq T \sum_t r_t^2$ , we have

$$R_t \leq \sqrt{\frac{T \gamma_{T,\alpha}^{\theta_L}}{\alpha}} \left\{ C_3 C_{(g)}^{1/g} \nu_{\theta_L, T} + \varphi_{t,\alpha}^L + \tau_g^{-1} \left( C_{(g)} \left( \frac{\sigma^2}{\alpha(T-1) + \sigma^2} \right)^{g/2} \right) \nu_{\theta_L, T} \right\}.$$

The result follows since our definition of  $\varphi_{T,\alpha}^L$  and  $m_{a,t,\theta_t}$  ensures  $\varphi_{T,\alpha}^L \leq \sqrt{2C_2} \|f\|_{\mathcal{H}_{\theta^U}} +$

---

<sup>3</sup>This is the only situation where we require  $\alpha \leq 1$

$$2\sqrt{2}m_{\alpha,T,\theta^L}.$$

□

## F.6 Proof of Theorem 4.3

We follow the same notation as in the proof of Theorem 4.2, as the proof structure for the  $0 \leq g < 1$  case is very similar to the general  $g$  case. The only difficulty is we can no longer rely on the Jensen's inequality as outlined in (32), and we have to come up with a new way to upper bound  $I_{t,1,\alpha}^\theta(x^*) \leq C_3\alpha_{\theta,1,\alpha}^{\text{EI}}(x^*|\mathcal{D}_{t-1})$ .

To this end, recall the uniform concentration bound we derived in Theorem 4.2 that with probability  $1 - \delta$ ,

$$|\mu_{t-1,\alpha}(\mathbf{x}, \theta_t) - f(\mathbf{x})| \leq \varphi_{t,\alpha}^{\theta_t} \sigma_{t-1,\alpha}(x; \theta_t), \quad \forall t \in \mathcal{N}, x \in \mathcal{X}.$$

Given that  $k(x, x) \leq 1$  and  $\alpha_{\theta,1,\alpha}^{\text{EI}}(x^*|\mathcal{D}_{t-1}) = E[(f(x^*) - \mu_{\theta,\alpha}^+)_+|\mathcal{D}_{t-1}]$ , we have

$$\begin{aligned} I_{t,1,\alpha}^\theta(x^*) &\leq C_3 E[(f(x^*) - \mu_{\theta,\alpha}^+)_+|\mathcal{D}_{t-1}] \\ &\leq C_3 (\varphi_{t,\alpha}^{\theta_t})^{1-g} E[((f(x^*) - \mu_{\theta,\alpha}^+)_+)^g|\mathcal{D}_{t-1}] \\ &\leq C_3 (\varphi_{t,\alpha}^{\theta_t})^{1-g} \alpha_{\theta,g,\alpha}^{\text{EI}}(x_t|\mathcal{D}_{t-1}) \\ &\leq C_3 C_{(g)} (\varphi_{t,\alpha}^{\theta_t})^{1-g} \nu_\theta^g \sigma_{t-1,\alpha}^g(x; \theta_t), \end{aligned}$$

where we again define constant  $C_{(g)} := \frac{2^{g/2}\Gamma((g+1)/2)}{2\sqrt{\pi}}$  and apply and (III) of Lemma F.2 to derive the last inequality. When  $0 \leq g \leq 1$ , by the same argument at the end of Lemma F.5, we know  $\sigma_{t-1,\alpha}^2(x_t; \theta) \geq \frac{\sigma^2}{\alpha(t-1) + \sigma^2}$ . This implies

$$\sigma_{t-1,\alpha}^g(x_t, \theta_t) = \sigma_{t-1,\alpha}(x_t; \theta_t) \sigma_{t-1,\alpha}^{g-1}(x_t; \theta_t) \leq \sigma_{t-1,\alpha}(x_t; \theta_t) \left( \frac{\sigma^2}{\alpha(t-1) + \sigma^2} \right)^{(g-1)/2}.$$

As illustrated in the proof of Theorem 4.2, our choice of  $\nu_\theta$  ensures that the ratio of  $\frac{\varphi_{t,\alpha}^{\theta_t}}{\nu_{\theta_t}}$  is uniformly bounded by some constant  $C_4$ . Hence we have  $(\varphi_{t,\alpha}^{\theta_t})^{1-g} \nu_\theta^g = \left( \frac{\varphi_{t,\alpha}^{\theta_t}}{\nu_{\theta_t}} \right)^{1-g} \nu_{\theta_t} \leq C_4^{1/g} \nu_{\theta_t}$ . It follows

$$I_{t,1,\alpha}^\theta(x^*) \leq \sigma_{t-1,\alpha}(x_t; \theta_t) \left\{ C_3 C_4^{1-g} C_{(g)} \nu_\theta^g \left( \frac{\sigma^2}{\alpha(t-1) + \sigma^2} \right)^{(g-1)/2} \right\}.$$

For simplicity, define  $C'_{(g)} := C_3 C_4^{1-g} C_{(g)}$ . We can bound the simple regret for  $0 \leq g < 1$  case as

$$r_t \leq \sigma_{t-1,\alpha}(x_t; \theta_t) \left\{ C'_{(g)} \nu_{\theta_t}^g \left( \frac{\sigma^2}{\alpha(t-1) + \sigma^2} \right)^{(g-1)/2} + \varphi_{t,\alpha}^{\theta_t} + \tau_g^{-1} \left( C_{(g)} \left( \frac{\sigma^2}{\alpha(t-1) + \sigma^2} \right)^{g/2} \right) \nu_{\theta_t} \right\}. \quad (34)$$

Observe that this instantaneous regret has the same structure as in (33). Hence the bound

for the cumulative regret can proceed in the same fashion as in the proof of Theorem 4.2:

$$R_t \leq \sqrt{\frac{T\gamma_{T,\alpha}^{\theta_L}}{\alpha}} \left\{ C'_g \nu_{\theta_L, T}^g \left( \frac{\sigma^2}{\alpha(t-1) + \sigma^2} \right)^{(g-1)/2} + \varphi_{t,\alpha}^L + \tau_g^{-1} \left( C_g \left( \frac{\sigma^2}{\alpha(T-1) + \sigma^2} \right)^{g/2} \right) \nu_{\theta_L, T} \right\}.$$

## G Proof of Proposition 5.1

*Proof.* Define the residual

$$r_s := y_s - \mu_{s-1,1}(x_s) = f(x_s) + \varepsilon_s - \mu_{t-1,1}(x_s) = \varepsilon_s - e_s.$$

Squaring  $r_s$  yields  $r_s^2 = \varepsilon_s^2 + e_s^2 - 2\varepsilon_s e_s$ . Hence the MSE can be written as

$$\text{MSE}_t = \frac{1}{t} \sum_{s=1}^t \varepsilon_s^2 + \frac{1}{t} \sum_{s=1}^t e_s^2 - \frac{2}{t} \sum_{s=1}^t \varepsilon_s e_s.$$

In particular, Let  $d_s := \varepsilon_s^2 - \sigma^2$ . Then  $\mathbb{E}[d_s | \mathcal{F}_{s-1}] = \mathbb{E}[\varepsilon_s^2 | \mathcal{F}_{s-1}] - \sigma^2 = 0$  and  $\{d_s\}$  is a martingale difference. By the martingale LLN, we have  $\frac{1}{t} \sum_{s=1}^t d_s \xrightarrow{p} 0$  and hence  $\frac{1}{t} \sum_{s=1}^t \varepsilon_s^2 \xrightarrow{p} \sigma^2$ . Similarly, since  $\mathbb{E}[\varepsilon_s | \mathcal{F}_{s-1}] = 0$ , and  $\sup_s \mathbb{E}[e_s^2 \varepsilon_s^2] \leq (\sup_s |e_s|)^2 \sup_s \mathbb{E}[\varepsilon_s^2] < \infty$ , another application of the martingale LLN yields  $\sum_{s=1}^t \varepsilon_s e_s \xrightarrow{p} 0$ . It follows we may write

$$\text{MSE}_t = \sigma^2 + \frac{1}{t} \sum_{s=1}^t e_s^2 + o(1).$$

Under the calibration case (i), we have  $\frac{1}{t} \sum e_s^2 \rightarrow 0$ , so  $\text{MSE}_t \xrightarrow{p} \sigma^2$ . Under the misspecification case (ii), we have  $\frac{1}{t} \sum e_s^2 \rightarrow b^2$ , so  $\text{MSE}_t \xrightarrow{p} \sigma^2 + b^2$ . The result follows by realizing that  $\hat{\alpha}_t := \frac{\text{PV}_t + \hat{\sigma}_t^2}{\text{PV}_t + \text{MSE}_t}$ .  $\square$

## H Empirical behaviour of normalized regret under tempered g-EI

We consider the Gaussian process Bayesian optimization setup of Section 4.3, with an  $\alpha$ -tempered posterior and the  $g$ -EI acquisition function defined in equation (10). Recall that at iteration  $t$  the algorithm evaluates a design point  $x_t \in \mathcal{X}$  and observes  $y_t = f(x_t) + \varepsilon_t$ , while  $x^* \in \arg \max_{x \in \mathcal{X}} f(x)$  denotes a (near) global maximizer of the objective. The instantaneous, cumulative, and average regrets are

$$r_t = f(x^*) - f(x_t), \quad R_T = \sum_{t=1}^T r_t, \quad \bar{r}_T = \frac{R_T}{T}. \quad (35)$$

The regret bounds in Theorems 4.2 and 4.3 control  $R_T$  for the  $\alpha$ -posterior GP surrogate and  $g$ -EI rule in terms of the tempered information gain  $\gamma_{T,\alpha}^{\theta_L}$  defined in (12) and a constant

$\beta_{T,\alpha,g}$  that depends on  $(\alpha, g)$  and the kernel parameters:

$$R_T = O(\beta_{T,\alpha,g} \sqrt{\gamma_{T,\alpha}^{\theta_L} T/\alpha}), \quad \text{for all } T \in \mathbb{N}, \quad (36)$$

for  $g \geq 1$  (Theorem 4.2) and  $0 \leq g < 1$  (Theorem 4.3) under their respective assumptions. For all experiments in this section we use the same smooth, moderately multimodal black-box objective

$$f(x) = \sum_{j=1}^d \sin(2\pi x_j) \exp(-x_j^2), \quad x = (x_1, \dots, x_d)^\top \in [-1, 1]^d \subset \mathbb{R}^d.$$

Unless stated otherwise we take  $d = 2$ , so  $\mathcal{X} = [-1, 1]^2$ .

## H.1 Normalized average regret.

In our experiments we do not plot  $\bar{r}_t$  directly, but a scale-free *normalized average regret*:

$$D_t(\alpha, g) := \frac{\bar{r}_t(\alpha, g)}{\bar{r}_1(\alpha, g)} = \frac{\frac{1}{t} \sum_{s=1}^t r_s(\alpha, g)}{r_1(\alpha, g)}. \quad (37)$$

By definition  $D_1(\alpha, g) = 1$  for all  $(\alpha, g)$ . Values  $D_t(\alpha, g) < 1$  indicate that the average regret up to time  $t$  is smaller than at the first iteration, while  $D_t(\alpha, g) > 1$  indicates that the algorithm has, on average, not improved upon its initial performance. This normalization removes the overall scale of the regret (which depends on the particular test function) and allows us to compare the relative decay in  $t$  across different choices of  $(\alpha, g)$ .

## H.2 Fixed kernel experiment

We fix a black-box objective  $f$  on a bounded domain  $\mathcal{X} \subset \mathbb{R}^d$  and approximate its global maximizer  $x^*$  by dense random search on  $\mathcal{X}$ . The surrogate model is a Gaussian process with squared-exponential kernel

$$k_\theta(x, x') = \sigma_f^2 \exp\left(-\frac{\|x - x'\|_2^2}{2\ell^2}\right), \quad (38)$$

where in this first set of experiments we keep the kernel hyperparameters  $\theta = (\ell, \sigma_f^2, \sigma^2)$  *fixed* across all runs. The  $\alpha$ -tempered posterior is obtained by inflating the noise variance to  $\sigma^2/\alpha$ , as in the regret analysis. At each iteration, the next design point  $x_{t+1}$  is chosen by maximizing a Monte Carlo approximation of the  $g$ -EI acquisition function  $\alpha_{\theta, g, \alpha}^{\text{EI}(f)}$  in (10) on a dense candidate set. For each pair  $(\alpha, g)$  we run the algorithm for a fixed number of iterations  $T$  and average the resulting regrets over several random seeds.

We measure performance via the *normalized average regret*

$$D_t(\alpha, g) := \frac{\bar{r}_t(\alpha, g)}{\bar{r}_1(\alpha, g)} = \frac{\frac{1}{t} \sum_{s=1}^t r_s(\alpha, g)}{r_1(\alpha, g)}, \quad (39)$$

where  $r_t = f(x^*) - f(x_t)$  and  $\bar{r}_t = t^{-1} \sum_{s=1}^t r_s$ . By construction,  $D_1(\alpha, g) = 1$  for all  $(\alpha, g)$ ;

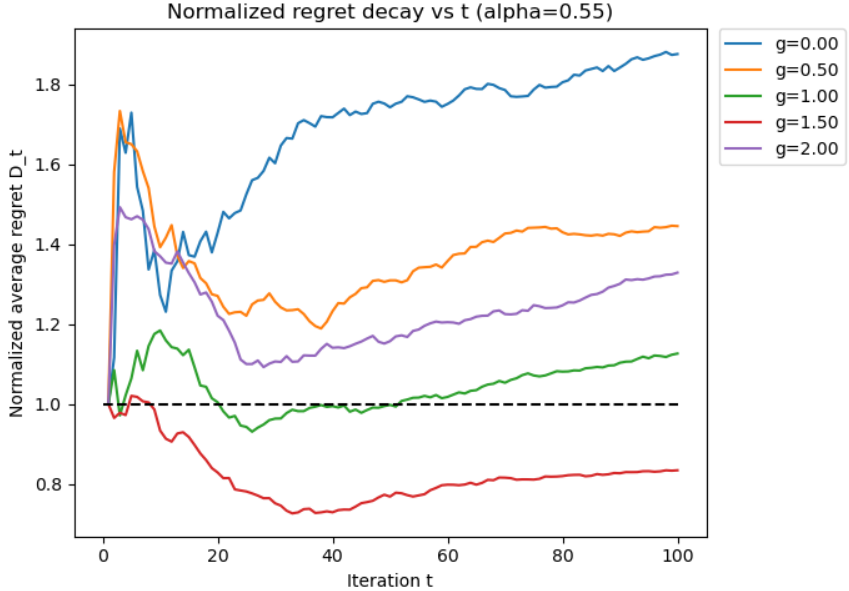


Figure 5: Normalized average regret  $D_t(\alpha, g)$  for fixed kernel parameters, with  $\alpha = 0.55$  and  $g \in \{0.0, 0.5, 1.0, 1.5, 2.0\}$ .

thus  $D_t(\alpha, g) < 1$  indicates that the average regret up to time  $t$  is smaller than at the first iteration, while  $D_t(\alpha, g) > 1$  indicates that the algorithm has, on average, not improved upon its initial performance.

**Effect of  $g$  at fixed  $\alpha$ .** Figure 5 reports  $D_t(\alpha, g)$  for a moderate tempering level  $\alpha = 0.55$  and  $g \in \{0.0, 0.5, 1.0, 1.5, 2.0\}$ . All curves start at  $D_1 = 1$ . The most exploitative choices,  $g = 0$  (PI) and  $g = 0.5$ , exhibit the largest normalized regrets: their curves rise above 1 and remain dominant over time. In contrast, the curves for  $g \geq 1$  are uniformly lower. This observation is consistent with Theorem 4.3, which shows that for  $0 \leq g < 1$  the regret bound acquires an additional factor  $T^{(1-g)/2}$ , strictly worsening the rate relative to the  $g \geq 1$  case. Among  $g \geq 1$ , the standard expected improvement ( $g = 1$ ) performs better than  $g = 2$ , in line with Theorem 4.2 which states that the dominant constant  $\beta_{T,\alpha,g}$  grows roughly like  $\sqrt{g}$  and cannot improve the asymptotic rate for  $g > 1$ . In this particular example  $g = 1.5$  performs slightly better than  $g = 1$  for the finite horizon considered; this does not contradict the theory, which provides worst-case upper bounds over all  $f$  in the RKHS and does not preclude a larger  $g$  from being beneficial for a specific test function and finite  $T$ .

**Effect of  $\alpha$  at fixed  $g$ .** Figure 6 shows  $D_t(\alpha, g)$  for the expected improvement rule  $g = 1$  and  $\alpha \in \{0.10, 0.33, 0.55, 0.78, 1.00\}$ . Again, all curves satisfy  $D_1 = 1$ . The untempered posterior  $\alpha = 1.0$  lies in the middle of the pack, whereas extreme tempering  $\alpha = 0.10$  performs the worst. The best empirical performance is obtained for a *moderate* level of tempering ( $\alpha \approx 0.55$ ), which dominates both  $\alpha = 1$  and more aggressive tempering in terms of normalized regret.

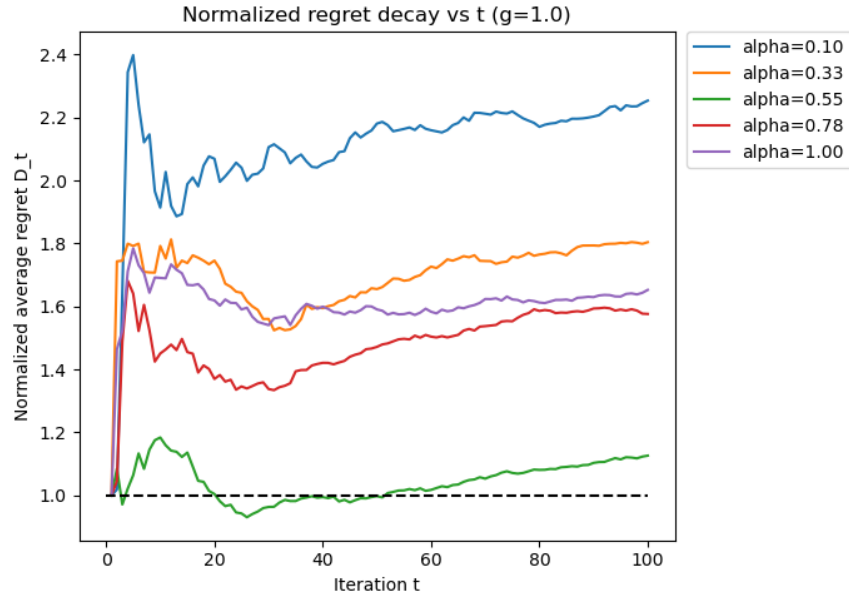


Figure 6: Normalized average regret  $D_t(\alpha, g)$  for fixed kernel parameters, with  $g = 1$  and  $\alpha \in \{0.10, 0.33, 0.55, 0.78, 1.00\}$ .

Theorem 4.2 predicts that the leading term in the regret bound

$$R_T(\alpha, g) = O\left(\beta_{T,\alpha,g} \sqrt{\gamma_{T,\alpha}^{\theta_L} T/\alpha}\right)$$

is an increasing function of  $\alpha$  for large  $T$ : the tempered information gain  $\gamma_{T,\alpha}^{\theta_L}$  is increasing and concave in  $\alpha$ , and the constant  $\beta_{T,\alpha,g}$  is also increasing in  $\alpha$  once the explicit  $\sqrt{\alpha}$  factor in  $m_{\alpha,T}^{\theta}$  has been factored out. Thus, the worst-case bound favours smaller  $\alpha < 1$  over the standard choice  $\alpha = 1$ . Our experiment supports this qualitative conclusion in that a suitably tempered posterior ( $\alpha \approx 0.55$ ) clearly outperforms  $\alpha = 1$  for  $g = 1$ . At the same time, the non-monotone behaviour across very small  $\alpha$  (e.g.  $\alpha = 0.10$ ) reflects the fact that Theorem 4.2 provides a *worst-case, asymptotic* guarantee over all functions in the RKHS; it does not imply that empirical regret will be monotone in  $\alpha$  for a fixed, finite-horizon problem. In practice, overly small  $\alpha$  inflate the effective noise variance  $\sigma^2/\alpha$  and can lead to excessive exploration and poor finite-sample performance.

Overall, these fixed-kernel experiments are qualitatively consistent with Theorems 4.2 and 4.3: (i) lowering  $g$  below 1 degrades regret, in line with the extra  $T^{(1-g)/2}$  factor in Theorem 4.3; (ii) moderate tempering  $\alpha < 1$  can substantially improve performance over the standard posterior, as suggested by the  $\alpha$ -dependence in Theorem 4.2; and (iii) very large  $g$  or very small  $\alpha$  may worsen finite-sample performance even if the corresponding worst-case bounds are not dramatically different.

### H.3 MLE-estimated kernel experiment

The theoretical analysis in Theorems 4.2 and 4.3 assumes a fixed kernel parameter  $\theta$ . In practice, however, Gaussian-process surrogates are often fit by maximizing the marginal likelihood with respect to  $\theta$  at each iteration. To assess the robustness of our conclusions

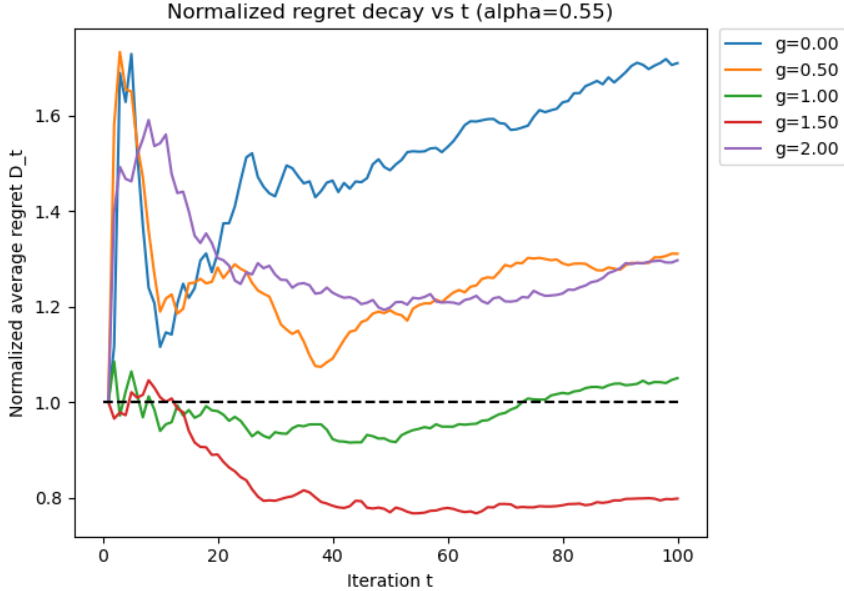


Figure 7: Normalized average regret  $D_t(\alpha, g)$  with MLE-estimated kernel parameters, for  $\alpha = 0.55$  and  $g \in \{0.0, 0.5, 1.0, 1.5, 2.0\}$ . The dashed horizontal line marks the baseline  $D_t = 1$ .

under such a more realistic modelling choice, we repeat the previous experiment but now *re-estimate* the kernel hyperparameters  $\theta = (\ell, \sigma_f^2, \sigma^2)$  at every BO step by maximizing the  $\alpha$ -tempered GP log marginal likelihood.

That is, given data  $(x_i, y_i)_{i=1}^t$  we choose

$$\hat{\theta}_t \in \arg \max_{\theta} \log p_{\alpha}(y_{1:t} \mid x_{1:t}, \theta),$$

where  $p_{\alpha}$  denotes the Gaussian-process model with effective noise variance  $\sigma^2/\alpha$ , and then use the corresponding posterior as our surrogate at iteration  $t + 1$ . The rest of the experimental design (domain, objective, candidate set, and computation of  $D_t(\alpha, g)$ ) is identical to the fixed-kernel case.

**Effect of  $g$  at fixed  $\alpha$  with MLE kernels.** Figure 7 reports  $D_t(\alpha, g)$  for  $\alpha = 0.55$  and the same range of  $g$  as in the fixed-kernel experiment. The qualitative ordering of the curves is unchanged:  $g = 0$  and  $g = 0.5$  perform the worst, while all  $g \geq 1$  obtain substantially lower normalized regrets. The curve for  $g = 1.5$  remains the best for this particular test function and horizon, followed by  $g = 1$  and  $g = 2$ . This confirms that the main message of Theorems 4.2 and 4.3 regarding the detrimental effect of  $g < 1$  persists even when the kernel parameters are not fixed but are re-estimated from data.

**Effect of  $\alpha$  at fixed  $g$  with MLE kernels.** Figure 8 shows  $D_t(\alpha, g)$  for  $g = 1$  under MLE-estimated kernels. As in the fixed-kernel case, a moderate tempering level  $\alpha \approx 0.55$  yields the lowest normalized regrets, staying below the baseline  $D_t = 1$  for the majority of the horizon. Extremely small  $\alpha = 0.10$  again performs poorly, while the untempered posterior  $\alpha = 1.0$  sits in the middle. Thus, the empirical support for the theoretical advantage

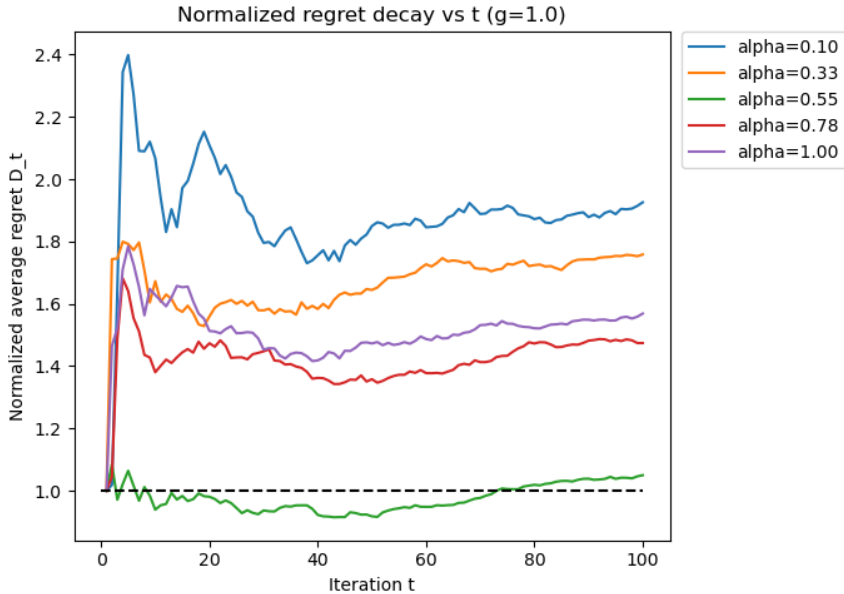


Figure 8: Normalized average regret  $D_t(\alpha, g)$  with MLE-estimated kernel parameters, for  $g = 1$  and  $\alpha \in \{0.10, 0.33, 0.55, 0.78, 1.00\}$ . The dashed horizontal line marks the baseline  $D_t = 1$ .

of tempering suggested by Theorem 4.2 is robust to whether the kernel hyperparameters are fixed or estimated by marginal likelihood.

Overall, re-estimating the kernel hyperparameters at each iteration leaves the qualitative conclusions of Section H.2 unchanged. The MLE-based experiments strengthen the practical relevance of the theory: in a setting that more closely matches typical GP-based Bayesian optimization pipelines, small  $g < 1$  and extreme tempering still harm performance, while moderate  $\alpha < 1$  combined with  $g$  near 1 remains a robust choice.

## I Simulation Results

We present our extensive simulation results across all configurations of the 61 functions, choices of  $g \in \{0, 1, 2\}$ , and choices of  $\alpha \in \{\text{tempered}, 1\}$ . The exact functional forms can be found in (Surjanovic and Bingham). Given the large experimentation size, we divide our visualizations based on the types of acquisition functions: probability of improvement ( $g = 0$ ), expected improvement ( $g = 1$ ), and the more explorative  $g = 2$  setting. For each table, we report the best average observed values across 5 seeds for the standard posterior ( $\alpha = 1$ ) and the tempered posterior.

The main empirical takeaway from these tables is that tempering the posterior can substantially improve Bayesian optimization performance in less exploratory settings, particularly when  $g$  is small and the acquisition function tends to overexploit. In contrast, tempering may become detrimental in more explorative configurations, such as when  $g = 2$ , where the posterior is already sufficiently dispersed. In such cases, additional tempering can lead to excessive exploration, slowing convergence. In below we used abbreviations “Dim” (for dimension of the input domain), “Avg Best Obs” (for average best black-box

function value observed during BO, across 5 seeds) for  $\alpha = 1$  (no tempering) and our schedule (9), for formatting purpose.

## I.1 Probability Improvement ( $g = 0$ )

Table 6: Aggregate performance by function and dimension, conditional on  $g = 0$ .

Function	Dim	Avg Best Obs ( $\alpha = 1$ )	Avg Best Obs (tempered)
ackley	5	-3.452	-3.321
ackley	10	-2.491	-2.325
alpine1	5	-1.438	-0.413
alpine1	10	-2.080	-1.253
beale	2	-0.659	-0.588
bohachevsky1	2	-108.105	-93.214
booth	2	-0.122	-0.066
branin	2	-0.127	-0.443
bukin6	2	-4.874	-5.929
camel3	2	-0.024	-0.237
camel6	2	-0.112	-0.171
colville	4	-164.696	-24.600
cross.in.tray	2	-0.049	-0.022
dejong5	2	-18.546	-29.812
dixon_price	5	-480.427	-285.579
dixon_price	10	-2072.582	-986.889
drop_wave	5	-0.763	-0.703
drop_wave	10	-0.833	-0.872
easom	2	-0.979	-0.979
eggholder	2	-386.309	-264.514
expanded_scaffer_f6	5	-2.029	-1.808
expanded_scaffer_f6	10	-4.252	-4.118
forrester08	1	-0.002	-0.003
goldstein_price	2	-44.358	-58.349
griewank	5	-1.666	-1.069
griewank	10	-2.918	-2.103
grlee12	5	-2.326	-2.736
grlee12	10	-5.721	-6.289
hartmann3	3	3.496	3.429
hartmann4	4	3.033	3.042
hartmann6	6	3.010	3.007
holder_table	2	-3.209	-2.992
levy	5	-2.087	-2.782
levy	10	-11.147	-8.815
levy13	2	-1.385	-2.480
matyas	2	-0.019	-0.006
mccormick	2	-0.177	-0.015

Function	Dim	Avg Best Obs ( $\alpha = 1$ )	Avg Best Obs (tempered)
Michalewicz	5	3.646	3.693
Michalewicz	10	5.208	5.407
powell	4	-27.853	-33.157
power_sum	4	-4.600	-9.743
rastrigin	5	-22.722	-23.701
rastrigin	10	-58.184	-46.369
rosenbrock	5	-20.584	-22.190
rosenbrock	10	-180.802	-63.301
rotated_hyper_ellipsoid	5	-165.625	-72.487
rotated_hyper_ellipsoid	10	-359.591	-414.822
schaffer2	2	-0.284	-0.250
schaffer4	2	-0.168	-0.165
schwefel	5	-813.596	-763.670
schwefel	10	-1803.187	-1881.817
shekel	4	2.334	2.867
shubert	2	-131.241	-117.361
sphere	5	-0.173	-0.156
sphere	10	-0.467	-0.430
styblinski_tang	5	-31.397	-33.645
styblinski_tang	10	-93.299	-94.053
sum_squares	5	-3.523	-1.733
sum_squares	10	-12.367	-8.927
zakharov	5	-32.609	-27.420
zakharov	10	-109.781	-88.803

## I.2 Expected Improvement ( $g = 1$ )

Table 7: Aggregate performance by function and dimension, conditional on  $g = 1$ .

Function	Dim	Avg Best Obs ( $\alpha = 1$ )	Avg Best Obs (tempered)
ackley	5	-1.737	-1.884
ackley	10	-2.820	-3.077
alpine1	5	-1.099	0.002
alpine1	10	-0.041	-0.138
beale	2	-1.154	-0.770
bohachevsky1	2	-14.524	-0.780
booth	2	-0.045	-0.013
branin	2	-0.018	-0.017
bukin6	2	-10.427	-10.878
camel3	2	-0.032	-0.036
camel6	2	-0.015	-0.018
colville	4	-1328.901	-1135.162

Function	Dim	Avg Best Obs ( $\alpha = 1$ )	Avg Best Obs (tempered)
cross_in_tray	2	-0.024	-0.002
dejong5	2	-67.646	-12.911
dixon_price	5	-138.061	-144.601
dixon_price	10	-517.435	-751.285
drop_wave	5	-0.726	-0.755
drop_wave	10	-0.878	-0.869
easom	2	-0.979	-0.979
eggholder	2	-182.684	-133.087
expanded_scaffer_f6	5	-1.740	-1.907
expanded_scaffer_f6	10	-4.177	-4.046
forrester08	1	0.004	0.004
goldstein_price	2	-21.052	-23.199
griewank	5	-1.178	-1.427
griewank	10	-1.485	-2.036
grlee12	5	-3.115	-3.278
grlee12	10	-6.654	-6.429
hartmann3	3	3.866	3.860
hartmann4	4	3.078	3.046
hartmann6	6	2.969	3.026
holder_table	2	-2.422	-1.934
levy	5	-2.443	-1.551
levy	10	-3.254	-3.921
levy13	2	-0.633	-0.610
matyas	2	-0.019	-0.019
mccormick	2	-0.005	-0.014
michalewicz	5	2.705	2.730
michalewicz	10	4.099	4.175
powell	4	-66.221	-51.681
power_sum	4	-64.558	-40.597
rastrigin	5	-40.644	-32.765
rastrigin	10	-80.757	-74.712
rosenbrock	5	-12.889	-10.043
rosenbrock	10	-55.403	-52.528
rotated_hyper_ellipsoid	5	-16.030	-60.150
rotated_hyper_ellipsoid	10	-1144.918	-86.920
schaffer2	2	-0.352	-0.359
schaffer4	2	-0.139	-0.150
schwefel	5	-855.969	-834.097
schwefel	10	-2012.762	-2362.358
shekel	4	1.922	2.306
shubert	2	-126.802	-142.241
sphere	5	-0.124	-0.162
sphere	10	-0.271	-0.222
styblinski_tang	5	-54.984	-50.817

Function	Dim	Avg Best Obs ( $\alpha = 1$ )	Avg Best Obs (tempered)
styblinski_tang	10	-150.483	-158.897
sum_squares	5	-1.171	-0.942
sum_squares	10	-4.403	-23.505
zakharov	5	-77.656	-61.315
zakharov	10	-250.712	-246.222

### I.3 Generalized Expected Improvement ( $g = 2$ )

Table 8: Aggregate performance by function and dimension, conditional on  $g = 2$ .

Function	Dim	Avg Best Obs ( $\alpha = 1$ )	Avg Best Obs (tempered)
ackley	5	-1.687	-2.133
ackley	10	-3.851	-3.554
alpine1	5	-0.005	-0.005
alpine1	10	-0.109	-0.169
beale	2	-0.853	-2.220
bohachevsky1	2	-5.783	-6.215
booth	2	-0.051	-0.054
branin	2	-0.031	-0.051
bukin6	2	-8.997	-7.316
camel3	2	-0.025	-0.043
camel6	2	-0.121	-0.292
colville	4	-1649.230	-1585.684
cross.in.tray	2	-0.013	-0.053
dejong5	2	-60.872	-123.331
dixon_price	5	-173.114	-203.670
dixon_price	10	-524.506	-631.709
drop_wave	5	-0.633	-0.635
drop_wave	10	-0.881	-0.840
easom	2	-0.979	-0.979
eggholder	2	-172.540	-253.179
expanded_scaffer_f6	5	-1.969	-1.900
expanded_scaffer_f6	10	-4.302	-4.222
forrester08	1	0.005	0.005
goldstein_price	2	-27.333	-9.885
griewank	5	-1.541	-1.562
griewank	10	-1.929	-2.103
grlee12	5	-2.940	-3.201
grlee12	10	-7.068	-6.578
hartmann3	3	3.821	3.844
hartmann4	4	3.059	3.003
hartmann6	6	2.888	2.780

Function	Dim	Avg Best Obs ( $\alpha = 1$ )	Avg Best Obs (tempered)
holder_table	2	-1.980	-1.959
levy	5	-1.655	-3.170
levy	10	-3.452	-3.796
levy13	2	-0.471	-0.465
matyas	2	-0.011	-0.013
mccormick	2	-0.023	-0.023
michalewicz	5	2.514	2.837
michalewicz	10	4.107	4.082
powell	4	-49.286	-74.269
power_sum	4	-68.390	-48.280
rastrigin	5	-27.716	-36.338
rastrigin	10	-83.323	-94.106
rosenbrock	5	-32.948	-21.622
rosenbrock	10	-88.737	-62.042
rotated_hyper_ellipsoid	5	-20.202	-35.040
rotated_hyper_ellipsoid	10	-101.289	-92.582
schaffer2	2	-0.358	-0.393
schaffer4	2	-0.148	-0.148
schwefel	5	-1018.261	-788.695
schwefel	10	-2218.329	-2561.653
shekel	4	1.326	1.389
shubert	2	-114.893	-114.971
sphere	5	-0.160	-0.163
sphere	10	-0.387	-0.580
styblinski_tang	5	-61.961	-61.637
styblinski_tang	10	-172.162	-186.270
sum_squares	5	-0.843	-0.791
sum_squares	10	-22.609	-35.938
zakharov	5	-68.837	-63.766
zakharov	10	-227.714	-250.555